4-2017

Tumor Necrosis Factor Alpha-Induced Recruitment of Inflammatory Mononuclear Cells Leads to Inflammation and Altered Brain Development in Murine Cytomegalovirus-Infected Newborn Mice

Maria C. Seleme
University of Alabama at Birmingham

Kate Kosmac
University of Kentucky, kate.kosmac@uky.edu

Stipan Jonjic
University of Rejika, Croatia

William J. Britt
University of Alabama at Birmingham

Tumor Necrosis Factor Alpha-Induced Recruitment of Inflammatory Mononuclear Cells Leads to Inflammation and Altered Brain Development in Murine Cytomegalovirus-Infected Newborn Mice

Notes/Citation Information
Published in *Journal of Virology*, v. 91, issue 8, e01983-16, p. 1-22.

Digital Object Identifier (DOI)
https://doi.org/10.1128/JVI.01983-16

AMERICAN SOCIETY FOR MICROBIOLOGY | Journal of Virology®

Tumor Necrosis Factor Alpha-Induced Recruitment of Inflammatory Mononuclear Cells Leads to Inflammation and Altered Brain Development in Murine Cytomegalovirus-Infected Newborn Mice

Maria C. Seleme,[b] Kate Kosmac,[a]* Stipan Jonjic,[d] William J. Britt[a,b,c]

Department of Microbiology, University of Alabama at Birmingham,[a] Department of Pediatrics Infectious Disease, University of Alabama at Birmingham,[b] Department of Neurobiology, University of Alabama at Birmingham, and University of Alabama School of Medicine,[c] Birmingham, Alabama, USA; Department of Embryology and Histology, University of Rejika Medical School, Rejika, Croatia[d]

ABSTRACT Congenital human cytomegalovirus (HCMV) infection is a significant cause of abnormal neurodevelopment and long-term neurological sequelae in infants and children. Resident cell populations of the developing brain have been suggested to be more susceptible to virus-induced cytopathology, a pathway thought to contribute to the clinical outcomes following intrauterine HCMV infection. However, recent findings in a newborn mouse model of the infection in the developing brain have indicated that elevated levels of proinflammatory mediators leading to mononuclear cell activation and recruitment could underlie the abnormal neurodevelopment. In this study, we demonstrate that treatment with tumor necrosis factor alpha (TNF-α)-neutralizing antibodies decreased the frequency of $CD45^+$ $Ly6C^{hi}$ $CD11b^+$ $CCR2^+$ activated myeloid mononuclear cells (MMCs) and the levels of proinflammatory cytokines in the blood and the brains of murine CMV-infected mice. This treatment also normalized neurodevelopment in infected mice without significantly impacting the level of virus replication. These results indicate that TNF-α is a major component of the inflammatory response associated with altered neurodevelopment that follows murine CMV infection of the developing brain and that a subset of peripheral blood myeloid mononuclear cells represent a key effector cell population in this model of virus-induced inflammatory disease of the developing brain.

IMPORTANCE Congenital human cytomegalovirus (HCMV) infection is the most common viral infection of the developing human fetus and can result in neurodevelopmental sequelae. Mechanisms of disease leading to neurodevelopmental deficits in infected infants remain undefined, but postulated pathways include loss of neuronal progenitor cells, damage to the developing vascular system of the brain, and altered cellular positioning. Direct virus-mediated cytopathic effects cannot explain the phenotypes of brain damage in most infected infants. Using a mouse model that recapitulates characteristics of the brain infection described in human infants, we have shown that TNF-α plays a key role in brain inflammation, including recruitment of inflammatory mononuclear cells. Neutralization of TNF-α normalized neurodevelopmental abnormalities in infected mice, providing evidence that virus-induced inflammation is a major component of disease in the developing brain. These results suggest that interventions limiting inflammation associated with the infection could potentially improve the neurologic outcome of infants infected *in utero* with HCMV.

Received 13 October 2016 **Accepted** 6 January 2017

Accepted manuscript posted online 25 January 2017

Citation Seleme MC, Kosmac K, Jonjic S, Britt WJ. 2017. Tumor necrosis factor alpha-induced recruitment of inflammatory mononuclear cells leads to inflammation and altered brain development in murine cytomegalovirus-infected newborn mice. J Virol 91:e01983-16. https://doi.org/10.1128/JVI.01983-16.

Editor Klaus Frueh, Oregon Health and Science University

Address correspondence to William J. Britt, wbritt@peds.uab.edu.

* Present address: Kate Kosmac, College of Health Sciences, University of Kentucky, Lexington, Kentucky, USA.

M.C.S. and K.K. contributed equally to this work.

KEYWORDS congenital infections, cytomegalovirus, neurodevelopment, tumor necrosis factor

Human cytomegalovirus (HCMV) infection, the most common viral infection acquired by the developing fetus, occurs in approximately 0.5 to 1% of live births in the United States and is an important cause of brain injury in infants and children (1). Although the clinical spectrum of neurologic disease following congenital HMCV infection is well documented, the variability in the phenotypes of central nervous system (CNS) sequelae coupled with limited availability of pathological specimens has resulted in an incomplete understanding of the mechanism(s) of CNS disease. The susceptibility of the developing CNS to CMV infection has been suggested to be a determinant of pathogenic outcomes in humans and animal models (2–18). In rodent models, CNS structural damage is associated with infection early in development (19). Similarly, human studies have suggested that maternal infection early in gestation is more commonly associated with structural damage in the brains of infected infants (20, 21). However, clinical studies have indicated that significant structural brain abnormalities are present in only a minority of infants with CNS sequelae following congenital HCMV infection, suggesting that mechanisms of disease other than the loss of CNS parenchyma are operative in the majority of infected infants (1, 22). Additionally, transmission of HCMV to the fetus occurs more frequently during the later stages of gestation, when the morphogenesis of major regions of the brain is nearly complete (20). Together, these observations suggest that CNS disease and long-term sequelae in the majority of infants with congenital HCMV infection likely arise from mechanisms other than direct viral cellular damage and loss of parenchyma in the developing brain.

Histological studies of tissue from fetuses and infants with fatal congenital HCMV have demonstrated mononuclear cell (MNC) infiltrates in the CNS, suggesting that host inflammatory responses contribute to the pathogenesis of infection (11, 23–25). Moreover, these studies also described a limited number of virus-infected cells within the CNS, indicating that virus-induced cellular cytopathology cannot account for the global and, importantly, the symmetric involvement of the brain in congenitally infected infants (11, 23–25). We have previously described a murine model of congenital HCMV infection in which newborn mice infected peripherally with nonlethal inocula of murine cytomegalovirus (MCMV) develop focal encephalitis with histological findings nearly indistinguishable from those reported in congenitally infected human infants (26, 27). Although focal infection can be found in all regions of the brain, MCMV-infected newborn mice exhibit measurable abnormalities in CNS development that are most readily observed in the cerebellum, presumably because that region of the murine brain undergoes extensive development during the time frame of MCMV infection in this model (26, 27). In the model, we have described a robust inflammatory response in the brains of MCMV-infected mice characterized by the infiltration of activated mononuclear cells and the expression of a large number of proinflammatory cytokines and interferon-regulated genes (IRGs) (26, 28). More recently, we demonstrated that corticosteroid treatment of infected mice decreased inflammation and normalized abnormalities in CNS development (29). Importantly, treatment did not alter the levels of virus replication in the CNS of infected mice during the time frame of treatment, suggesting that inflammation induced by infection, and not virus-induced cytopathology, was responsible for developmental abnormalities in the brain (29). While the specific targets of the anti-inflammatory effects of corticosteroid treatment in the model remain undefined, infection-induced soluble inflammatory mediators, including tumor necrosis factor alpha (TNF-α), gamma interferon (IFN-γ), and IFN-β, were decreased (29). Because of the potential toxicity of corticosteroids for the developing CNS, as well as the off-target effects of corticosteroids that have been documented in clinical studies and in animal models, we sought more targeted approaches to decrease CNS inflammation in infected mice (30–32). We focused our studies on responses associated

with TNF-α because pathway analyses of the transcriptome from cerebella of infected mice revealed that TNF-α represented a central node in the pathway of the observed inflammatory responses (26).

TNF-α is induced following MCMV infection and can function in the control of virus replication (33–36). A direct antiviral effect of TNF-α on CMV replication in primary human astrocytes has been documented *in vitro* (37). Indirect mechanisms responsible for the antiviral activities of TNF-α in MCMV-infected mice have also been proposed, such as facilitating the infiltration of monocytes/macrophages and $CD8^+$ T lymphocytes into sites of infection and increasing mononuclear cell activation (38, 39). Similarly, in other viral infections, TNF-α has also been shown to have a protective role. The results from studies in a murine model of viral encephalitis have shown that TNF-α facilitates recruitment of monocytes/macrophages into the CNS of West Nile virus (WNV)-infected mice (38). Treatment of infected mice with neutralizing TNF-α antibodies increased the mortality in infected mice, suggesting an important role for TNF-α early in the control of virus infection in the brain, presumably through its effect on the recruitment of inflammatory monocyte/macrophage populations (38). TNF-α has also been shown to be protective in murine models of herpes simplex virus (HSV) encephalitis and in clearance of lymphocytic choriomeningitis virus (LCMV) (40, 41). In contrast to these findings, other studies have argued that TNF-α facilitates WNV neuroinvasion by disrupting the integrity of the blood-brain barrier, a mechanism that may also contribute to increases in mononuclear cell infiltration into the infected CNS (42). In contrast to antiviral responses, TNF-α expression in the CNS has also been associated with both neurodegenerative and neurodevelopmental diseases. Both direct and indirect neurotoxic effects of TNF-α in culture systems have been reported, and TNF-α has been proposed to contribute to neurodegeneration observed in HIV-associated dementia (43–50). Transgenic mice constitutively expressing TNF-α in the CNS exhibit severe inflammation and associated histopathological findings, including microgliosis with infiltrating macrophages (51). Importantly, histological changes in these mice were modified by peripheral administration of a TNF-α-neutralizing antibody (TNF-NAb) (51). Neuronal overexpression of TNF-α has been associated with increased cytokine production and lower seizure thresholds in Borna virus-infected rodents (52). TNF-α neurotoxicity has been associated with the recruitment of inflammatory monocytes to sites of inflammation in the brain, similar to its pathogenic function in other organ systems (53, 54). Together, these studies suggest that a balance exists between protective host responses and pathogenic inflammation associated with TNF-α expression. Importantly, the balance between protective responses and disease is variable depending on the organ that is involved, and in the case of the brain, the developmental status of the brain during virus-induced inflammation.

In the present study, we used TNF-NAbs to explore the role of TNF-α in altered CNS development following MCMV infection of the developing CNS. MCMV-infected mice were treated with TNF-NAbs, and the effects on virus replication, the induction of inflammatory responses, and cerebellar development during the early postnatal period were determined. Our findings indicated that neutralization of TNF-α did not significantly alter the levels of virus replication during the time interval of our experiments but decreased CNS inflammation associated with MCMV infection. Notably, neutralization of TNF-α resulted in a significant decrease in activated blood myeloid mononuclear cells (MMCs) ($CD45^{int}$ $Ly6C^{hi}$ $CD11b^+$ $CCR2^+$) that trafficked into the CNS, suggesting that the infiltration of these cells into the CNS of MCMV-infected mice was a major component of inflammation in the brains of MCMV-infected newborn mice. Moreover, treatment of infected mice with TNF-NAb normalized previously described developmental abnormalities in the cerebellum, providing further evidence that host inflammatory responses, specifically those associated with TNF-α, following MCMV infection were a major component of the mechanism(s) leading to alterations in developmental programs of the brain.

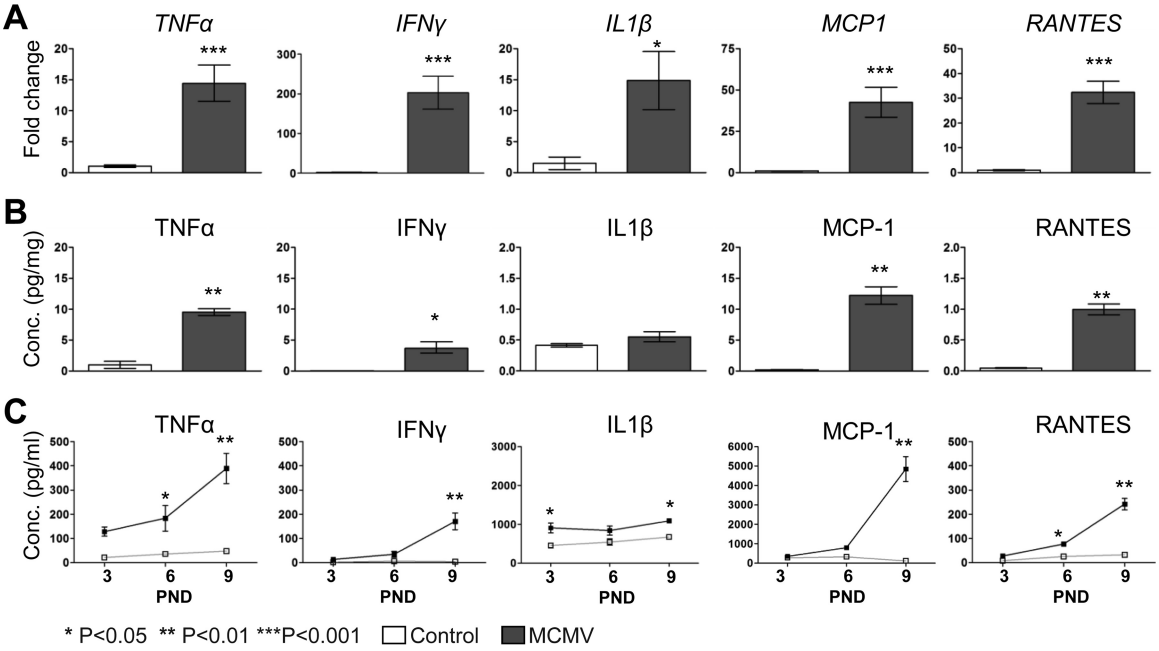

FIG 1 Increased inflammatory responses following MCMV infection of newborns. (A and B) Transcription (A) and protein levels (B) of proinflammatory mediators in the cerebella of control and MCMV-infected PND 8 mice. The *P* values were calculated using a two-tailed *t* test. (A) qPCR of cerebellar mRNA. The data are shown as mean fold changes ± standard errors of the mean (SEM) normalized to vehicle-treated control; $n = 5$ to 7 mice/group. (B) Cytokine/chemokine levels in cerebellar homogenates. The data are shown as medians with interquartile ranges; $n = 3$ cerebella/sample with 3 replicates/group. Conc., concentration. (C) Serum concentrations of cytokines/chemokines during acute infection. The data are shown as means ± SEM; $n = 3$ mice/group. The *P* values were calculated using two-way ANOVA with Bonferroni posttests.

RESULTS

TNF-NAb treatment of MCMV-infected newborn mice decreases the inflammatory response in the cerebellum without altering virus replication. MCMV infection of newborn mice results in hematogenous spread to the brain, with peak levels of virus in the brain detected on postnatal day (PND) 8 and the induction of proinflammatory responses in the brain that also peak on PND 8 (26, 29). We initially analyzed the transcription and protein levels of a subset of proinflammatory cytokines and chemokines involved in mononuclear cell recruitment and confirmed previously described increases in the transcription of the proinflammatory cytokine genes *TNF-α*, interleukin 1β (*IL-1β*), and *IFN-γ* and the chemokine genes *MCP-1* and *RANTES* in the cerebella of PND 8-infected mice (Fig. 1A) (26). Protein levels of TNF-α, MCP-1, RANTES, and IFN-γ were also increased in cerebella from MCMV-infected mice (Fig. 1B). Serum TNF-α, MCP-1, RANTES, IFN-γ, and, to a lesser extent, IL-1β levels also increased over the course of acute infection (Fig. 1C). The increased expression of chemokines associated with mononuclear cell recruitment to the CNS (MCP-1 and RANTES) was consistent with previous descriptions of the infiltration of myeloid and lymphoid cells into the CNS following MCMV infection (28, 29).

As was noted previously, pathway analysis, using commercially available software (Ingenuity; Qiagen), of the transcriptome derived from the cerebella of MCMV-infected mice indicated that TNF-α represented a critical regulatory molecule in the inflammatory responses (26, 28, 29). To define the role of TNF-α signaling in proinflammatory responses in the cerebellum, we treated MCMV-infected and uninfected (control) mice with TNF-NAbs on PND 4 to 7 and assayed the transcription of genes encoding proinflammatory molecules in the cerebella from PND 8 mice. The expression of *TNF-α*, as well as *IL-1β*, *MCP-1*, *RANTES*, *IFN-β*, *IFN-γ*, and *STAT1*, RNA was decreased in the cerebella of TNF-NAb-treated infected mice (Fig. 2A). Given the reported roles of *IFN-β*, *IFN-γ*, and *STAT1* in the control of virus replication, we expected that downstream genes involved in antiviral responses would also be decreased in the brains of infected

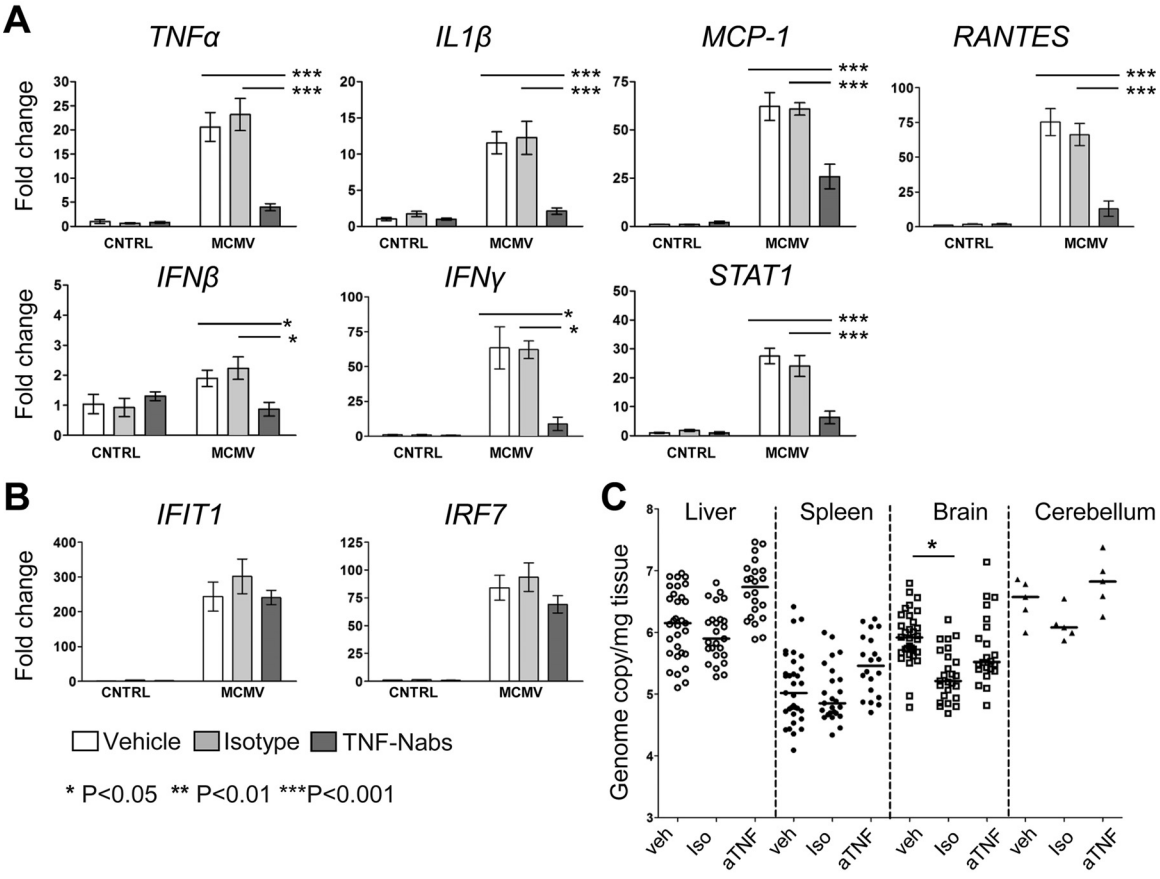

FIG 2 Treatment of MCMV-infected mice with TNF-NAbs decreases inflammatory responses in the cerebellum. (A and B) Transcription of proinflammatory cytokines and chemokines (A) and interferon-regulated genes (B) in the cerebella from control and MCMV-infected mice treated with vehicle or with isotype or TNF-NAbs. The fold change was normalized to the vehicle-treated control. The data are shown as means ± SEM. The *P* values were calculated by two-way ANOVA with Bonferroni posttests; $n = 5$ mice/group. (C) Median MCMV genome copy numbers ($\log_{10}$) in infected mice treated with vehicle or with isotype or TNF-NAbs. The *P* values were calculated using a Kruskal-Wallis test of medians with Dunn posttest correction; $n = 25$ to 35 mice/group for liver, spleen, and brain; $n = 5$ mice/group for cerebellum.

mice treated with TNF-NAbs; however, treatment had little effect on the transcription of *IFIT1* or *IRF7* in the cerebella of infected mice (Fig. 2B). Thus, in contrast to our previous results from studies using corticosteroid treatment to reduce CNS inflammation in infected mice, TNF-NAbs appeared to exhibit somewhat more specificity in the regulation of proinflammatory responses in the cerebella of MCMV-infected neonatal mice (29).

To determine if the reduction in the expression of proinflammatory molecules following neutralization of TNF-α was associated with increased virus replication in MCMV-infected mice, we quantified MCMV replication in the livers, spleens, and brains of infected mice (29). With the exception of a small decrease in viral DNA in the brains of infected mice treated with isotype control antibodies (IC), statistically insignificant changes in viral genome copy numbers were observed in the livers, spleens, brains, and cerebella of infected mice following TNF-NAb treatment compared to vehicle or isotype control antibody-treated infected animals (Fig. 2C). Together, these data indicated that treatment of MCMV-infected newborn mice with TNF-NAbs modulated inflammatory responses in the brain but did not result in a significant change in the levels of virus replication in multiple organs, including the brain cortex and cerebellum.

Neutralization of TNF-α corrects developmental deficits in the cerebella of MCMV-infected neonatal mice. To investigate the contribution of TNF-α to inflammation-associated abnormalities in CNS development following MCMV infection, we analyzed cerebellar morphogenesis in infected mice following TNF-NAb treatment. As we have reported previously, the cerebellar area, external granule cell layer (EGL) thickness, and

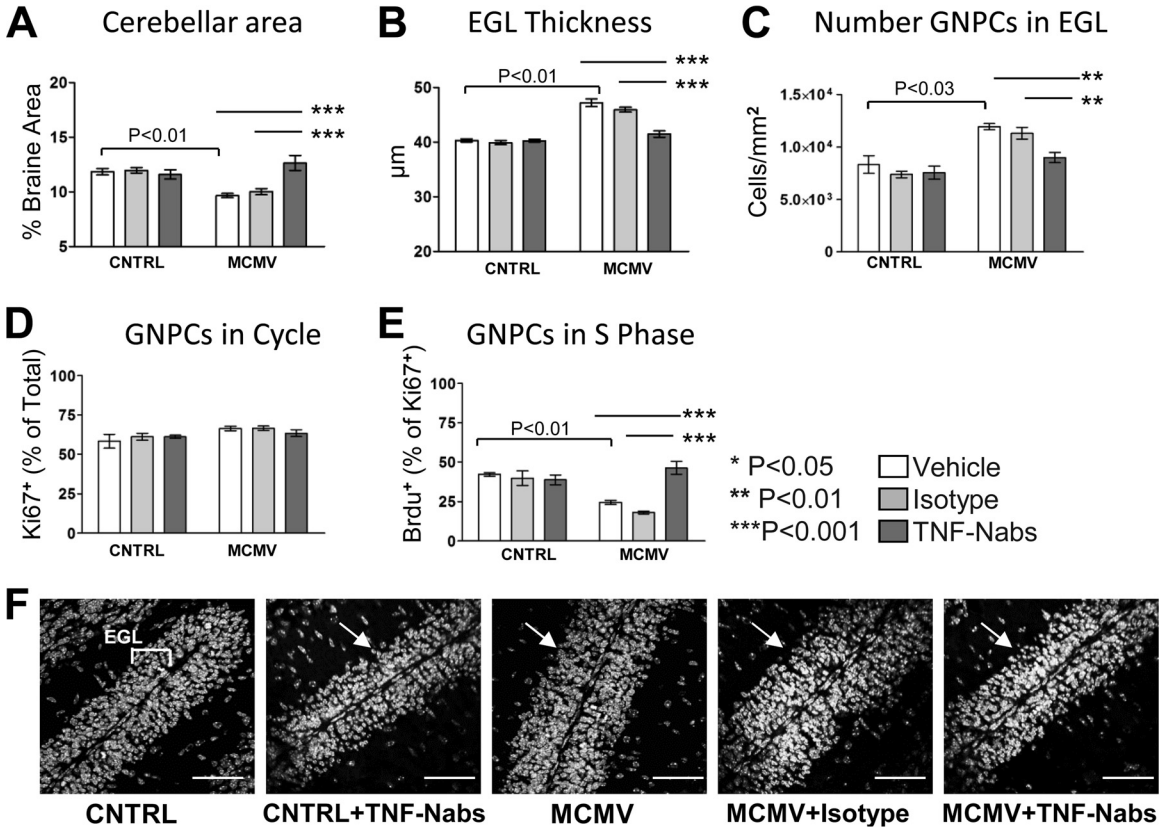

FIG 3 TNF-NAbs normalize abnormalities in cerebellar development following MCMV infection. (A) Cerebellar area of control for infected mice treated with vehicle or with isotype or TNF-NAbs. Five sections were analyzed/mouse; $n = 5$ mice/group. (B) Cerebellar EGL measurements from vehicle-, isotype-, or TNF-NAb-treated control and infected mice (32 measurements/mouse). (C) GNPC counts in the EGL of vehicle-, isotype-, and TNF-NAb-treated control and infected mice; 8 sections were analyzed/mouse. (D and E) Quantification of $Ki67^+$ (D) and $BrdU^+$ (E) GNPCs in the EGL of control and MCMV-infected mice treated with vehicle or with isotype or TNF-NAbs; 8 sections were analyzed/mouse. (B to E) $n = 3$ mice/group for vehicle- treated animals; $n = 5$ mice/group for isotype- or TNF-NAb-treated animals. The data are shown as means ± SEM. The *P* values were calculated by two-way ANOVA with Bonferroni posttests. (A to C and E) Vehicle-treated infected mice were significantly different ($P \leq 0.05$) from vehicle-treated control mice, as determined by two-tailed *t* test. (F) Representative confocal images showing the thickness of the EGL (arrow) following vehicle, isotype, or TNF-NAb treatment of control and MCMV-infected mice. Images, ×60 magnification.

granule neuron progenitor cell (GNPC) number were altered in MCMV-infected newborn mice compared to these values in uninfected control mice (Fig. 3A to C and F) (26, 29). Treatment of infected mice with TNF-NAbs resulted in the normalization of these morphological abnormalities (Fig. 3A to C and F). Importantly, treatment with TNF-NAbs had no effect on cerebellar morphogenesis in control animals (Fig. 3A to C and F). Similarly, treatment with isotype antibodies did not alter the abnormal cerebellar development observed in MCMV-infected mice or normal cerebellar development in control mice (Fig. 3A to C).

Previously we demonstrated that altered cerebellar morphogenesis in infected mice was associated with abnormalities in GNPC proliferation in the EGL of the cerebellar cortex. Altered GNPC proliferation was characterized by decreased bromodeoxyuridine (BrdU) incorporation without significant changes in the percentage of actively cycling ($Ki67^+$) GNPCs (29). Consistent with these results, fewer GNPCs were $BrdU^+$ in cerebella following MCMV infection, while the percentage of cycling ($Ki67^+$) GNPCs remained unchanged compared to control animals (Fig. 3D and E) (29). Treatment of infected mice with TNF-NAbs normalized the frequency of $BrdU^+$ GNPCs in the EGL (Fig. 3D and E). Treatment with isotype control antibodies had no effect on altered proliferation of cerebellar GNPCs following infection (Fig. 3D and E). These results strongly argued that neutralizing TNF-α with TNF-NAbs restored the proliferative capacity of GNPCs in the cerebella of MCMV-infected mice, likely contributing to the normalization of the

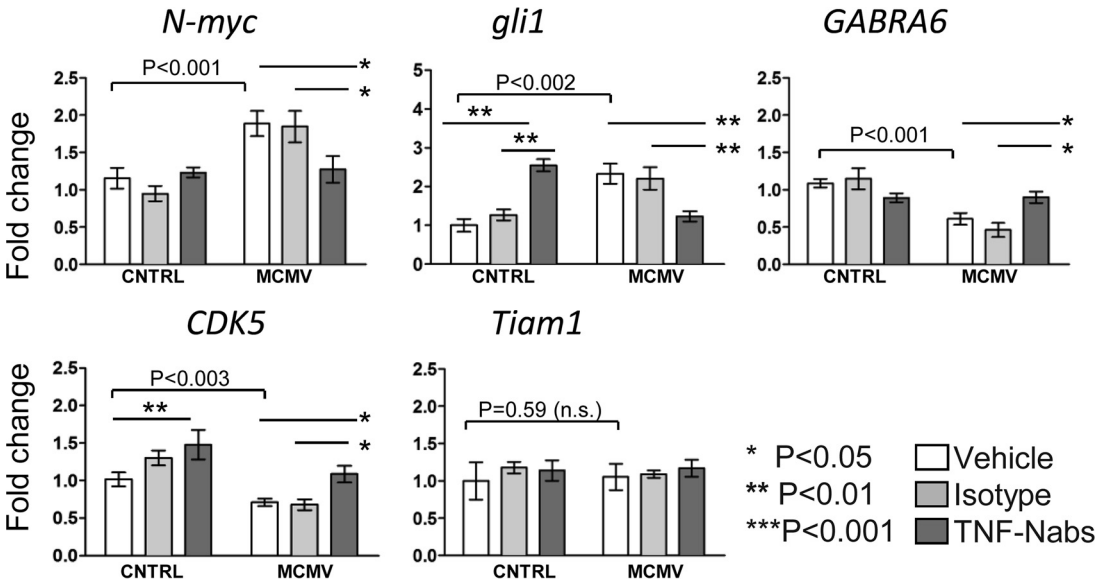

FIG 4 TNF-NAb treatment of MCMV-infected mice normalizes developmental gene expression in the cerebellum. Shown are transcription levels of developmentally regulated genes in the cerebella of vehicle-, isotype-, or TNF-NAb-treated control and infected mice. The data are shown as means ± SEM. Statistical significance was calculated using two-way ANOVA with Bonferroni posttest; $n = 5$ mice/group. Vehicle-treated infected mice were significantly different ($P \leq 0.05$) from vehicle-treated control mice as determined by two-tailed *t* test (excluding *Tiam1*). n.s., not significant.

parameters of cerebellar morphogenesis. No differences were observed in the percentage of cycling ($Ki67^+$) GNPCs entering S phase ($BrdU^+$) following isotype antibody or TNF-NAb treatment of control mice (Fig. 3D and E).

Morphological deficits in the cerebella of infected mice also coincided with altered transcription of several developmentally regulated genes within GNPCs. Corticosteroid treatment normalized transcription of these genes (26, 29). Consistent with these findings, the transcription of two genes used to monitor GNPC differentiation, *GABRA6* and *CDK5*, was decreased following infection (Fig. 4) (55–59). The expression of both *GABRA6* and *CDK5* was normalized in the cerebella of infected mice following TNF-NAb treatment (Fig. 4). In addition, transcription of *N-myc* and *gli1*, two genes in the sonic hedgehog (*Shh*) pathway of GNPC proliferation, was increased in the cerebella of infected mice (Fig. 4). Treatment with TNF-NAbs reduced the transcription of both genes to levels comparable to those in control mice (Fig. 4) (29). Treatment with isotype antibodies did not alter the transcription of these genes in the cerebella of control or infected mice (Fig. 4). No differences were noted in the expression of *gli1* or *CDK5* in control animals treated with vehicle or isotype control antibody; however, treatment with TNF-NAbs increased the expression of *gli1* and *CDK5* in control mice (Fig. 4). We have not determined the mechanism for this apparent off-target effect on *gli1* and *CDK5* expression in control mice treated with TNF-NAbs, but it is important to note that the effect was an increase in transcription above what was observed in vehicle-treated MCMV-infected mice. This result suggested that the effect was unrelated to the normalization (decreased expression) of *gli1* expression in MCMV-infected mice treated with TNF-NAbs (Fig. 4). Increased expression of *CDK5* in control animals following TNF-NAb treatment was not statistically different than *CDK5* expression in control animals treated with isotype control antibody, arguing that this off-target effect was not mediated specifically by TNF-NAbs (Fig. 4). As a control, the transcription of *Tiam1*, a guanine nucleotide exchange factor expressed in GNPCs during cerebellar development and involved in GNPC migration, was assayed (60, 61). Transcription of *Tiam1* remained unaltered across all experimental treatment groups, suggesting specificity in the observed transcriptional changes for gene pathways involved in GNPC proliferation. These data demonstrated that neutralizing TNF-α in infected mice normalized abnormalities in morphogenesis, GNPC proliferation, and developmental gene transcription

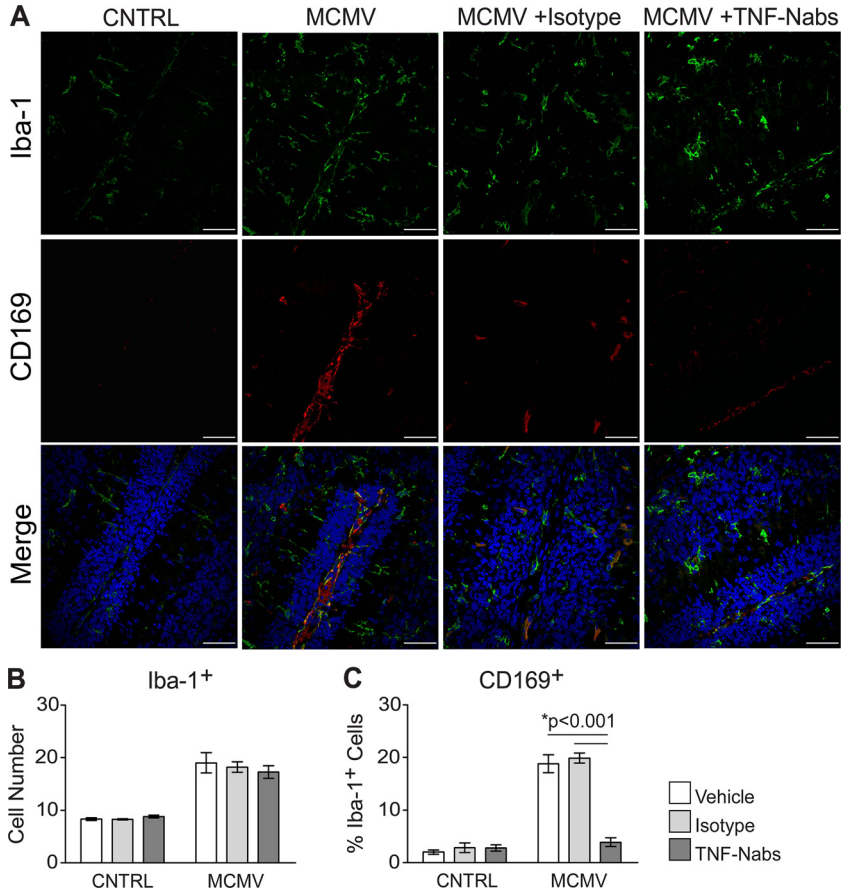

FIG 5 TNF-NAb treatment decreases CD169$^+$ Iba-1$^+$ monocytes in the CNS of MCMV-infected mice. (A) Immunofluorescence detection of Iba-1$^+$ (green), CD169$^+$ (red), and Hoechst (blue) cells in the cerebella of vehicle-treated control mice and vehicle-, isotype-, and TNF-NAb-treated infected mice analyzed by confocal microscopy. Magnification, ×40; scale bars = 50 μm. (B and C) Quantification of Iba-1$^+$ cells (B) and the percentages of CD169$^+$ cells within the Iba-1$^+$ population (C) in the cerebella of vehicle-, isotype-, or TNF-NAb-treated control and infected mice; 4 sections were counted/animal; n = 5 mice/group. The graphs show means ± SEM. The P values were calculated using two-way ANOVA with Bonferroni posttest.

in the cerebellum, supporting our hypothesis that TNF-α and/or downstream effectors contributed to the altered cerebellar development in MCMV-infected newborn mice.

TNF-NAb treatment of MCMV-infected mice results in decreased CNS infiltration of activated inflammatory monocytes, nonclassical monocytes, and lymphoid cells. Earlier studies in this model system demonstrated that focal mononuclear cell infiltrates were widely distributed throughout the brain, including the cerebellum, and often associated with MCMV-infected resident cells of the CNS (26, 62). The finding that treatment with TNF-NAbs decreased CNS inflammation and normalized cerebellar development in MCMV-infected newborn mice raised the possibility that TNF-NAbs limited CNS inflammation by decreasing mononuclear cellular infiltrates into the CNS of MCMV-infected mice, similar to our findings in a previous study in which corticosteroids were used to dampen inflammation (29). Cells of the myeloid lineage (Iba-1$^+$), including microglia, were identified in tissue sections from the brains of PND 8 mock- and MCMV-infected mice, as well as mice treated with TNF-NAbs. Significant increases in the numbers of Iba-1$^+$ cells in the brains of infected mice were observed compared to mock-infected mice, regardless of whether they were treated with TNF-NAbs (Fig. 5A and B). When the population of Iba-1$^+$ cells was further analyzed for the expression of CD169, a myeloid marker expressed by peripheral blood monocytes but not by resident microglia, we noted that approximately 20% of Iba-1$^+$ cells in cerebellar sections from

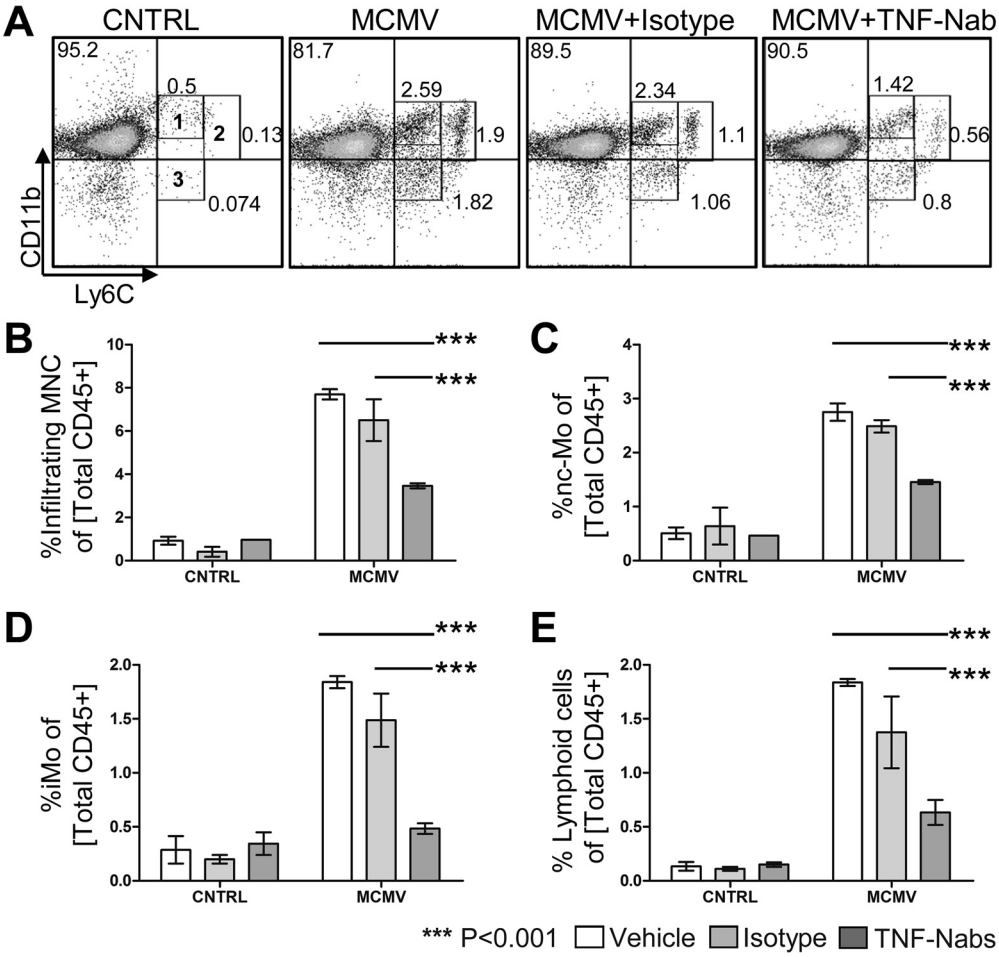

FIG 6 Decreased infiltration of myeloid and lymphoid cells in the CNS of MCMV-infected mice treated with TNF-NAb. (A) Representative flow cytometry dot plots showing the frequency of cells expressing CD11b$^+$ Ly6C$^+$ cells gated on total live CD45$^+$ mononuclear cells isolated from the brains of uninfected or MCMV-infected mice left untreated or treated with isotype or TNF-NAbs. The gates labeled 1, 2, and 3 in the uninfected (CNTRL) plot identify the nc-Mo and iMo subsets in the upper right quadrant and the lymphoid subset in the lower right quadrant. The numbers next to the gates correspond to representative percentages of each cell subset. (B to E) Quantifications depicting, out of total (CD45$^+$) MNCs, the percentages of total (Ly6C$^{int/hi}$) brain-infiltrating MNCs (B), nc-Mo (CD11b$^+$ Ly6C^{int}) (C), iMo (CD11b$^+$ Ly6C^{hi}) (D), and lymphoid cells (CD11b$^{low/-}$ Ly6C^{int}) (E). The data are shown as means ± SEM; $n = 2$ or 3 replicates, with 4 mice pooled per replicate. The P values were calculated using two-way ANOVA, with Bonferroni posttests.

MCMV-infected mice also expressed CD169 (Fig. 5A and C). Treatment of MCMV-infected mice with TNF-NAb significantly decreased the population of Iba-1$^+$ CD169$^+$ cells but only minimally decreased the total numbers of Iba-1$^+$ cells in the cerebella of infected mice (Fig. 5A and C). This finding suggested that TNF-NAbs could decrease inflammation in the CNS of infected mice by limiting recruitment of peripheral blood monocytes to the brains of MCMV-infected mice. Together, these results suggested that peripheral blood monocytes contributed to the immunopathology associated with MCMV infection in the developing brains of neonatal mice.

To further investigate the role of peripheral blood monocytes in the altered cerebellar development in MCMV-infected mice, we used flow cytometry to quantify MNCs isolated from the brains of treated and control animals. In these studies, we took advantage of the cell surface antigen Ly6C, which is differentially expressed in classical and nonclassical peripheral blood monocytes, natural killer (NK) cells, and subsets of activated lymphocytes (63–66). Importantly, previous studies have reported that Ly6C is not expressed by CNS-resident microglia (67). Resident microglia (Ly6C$^-$) and infiltrating MNCs (Ly6C$^+$) were distinguished by gating Ly6C with CD11b (Fig. 6A). Differ-

ential expression of Ly6C and CD11b in the infiltrating subset allowed the resolution of 3 subsets of mononuclear cells: myeloid patrolling or nonclassical monocytes that expressed CD11b and intermediate levels of Ly6C (nc-Mo) ($CD11b^+$ $Ly6C^{int}$) (Fig. 6A); classical or inflammatory monocytes expressing CD11b and the highest levels of Ly6C (iMo) ($CD11b^+$ $Ly6C^{hi}$) (Fig. 6A); and lymphoid cells, expressing intermediate levels of Ly6C and either low or nondetectable levels of the myeloid marker CD11b ($CD11b^{low/-}$ $Ly6C^{int}$) (Fig. 6A). The differential expression of CD45, a surface marker that has been used to differentiate between brain-resident ($CD11b^+$ $CD45^{int/lo}$) and infiltrating ($CD11b^+$ $CD45^{hi}$) MNC subsets in earlier studies, in brain MNCs was also noted (references 28, 29, and 68 and data not shown). Consistent with previous findings, MCMV infection induced a robust immune response in the neonatal brain, as indicated by an increase in the frequencies of both myeloid ($CD45^{int}$ $CD11b^+$ $Ly6C^{int/hi}$) and lymphoid ($CD45^{hi}$ $CD11b^{low/-}$ $Ly6C^{int}$) cells infiltrating the brain compared to uninfected controls (Fig. 6A and B). Further analysis of the $CD45^{hi}$ $CD11b^{low/-}$ $Ly6c^{int}$ subset revealed that about 50% of these cells were $NKp46^+$ $CD3^-$, indicating that they were NK cells (data not shown). Analysis of the individual infiltrating subsets revealed that after MCMV infection, the average frequencies of the nc-Mo, iMo, and lymphoid subsets increased 3.6-, 11.5-, and 12.8-fold, respectively, compared to the corresponding frequencies in uninfected mice (Fig. 6A, C, D, and E). In mice treated with TNF-NAbs, the frequency of infiltrating MNCs was decreased to approximately half of that of the average frequencies observed in untreated, infected animals (Fig. 6A and B). In infected mice treated with TNF-NAbs, infiltrating nc-Mo, iMo, and lymphoid subsets decreased by 54%, 71%, and 60%, respectively, relative to the respective frequencies in untreated, infected animals (Fig. 6C, D, and E). Mice treated with the IC exhibited a smaller, nonsignificant decrease in the same subsets of mononuclear cells. These results indicated that each MNC subset identified in the MCMV-infected brain infiltrate was significantly decreased following systemic treatment with TNF-NAbs (Fig. 6).

In murine models of CNS disease, either degenerative or as a result of viral infection, the infiltration of activated monocytes defined as blood-derived MNCs expressing $Ly6C^{hi}$ and CCR2 (iMo) has been associated with sustained inflammation and increased pathology (67, 69–74). We next analyzed the activation state of iMo infiltrating the CNS of MCMV-infected newborn mice before and after TNF-NAb treatment by measuring the expression of the CCR2 receptor, the major histocompatibility complex class II (MHC-II), and the costimulatory molecule CD80. Following MCMV infection, the average frequency of iMo in brains from infected mice that expressed MHC-II was 18.8%, whereas MHC-II was not detected in iMo from uninfected mice (Fig. 7A). Similarly, the frequencies of iMo expressing CD80 and CCR2 were increased 4.4- and 3.4-fold, respectively, compared to the frequencies of iMo expressing these markers in uninfected controls (Fig. 7C and E). The average median fluorescence intensity (MFI) values of MHC-II, CD80, and CCR2 were also increased over the average MFI values in cells from uninfected animals (Fig. 7B, D, and F). Importantly, following TNF-NAb treatment, the frequencies and MFI values of iMo expressing MHC-II, CD80, and CCR2 did not decrease significantly compared to untreated or IC-treated controls (Fig. 7). Thus, in this model system, TNF-NAb treatment significantly reduced the infiltration of MNCs into the brains of MCMV-infected mice, including the number of infiltrating iMo, but did not significantly alter the level of activation of iMo in the infected brain. These findings suggested that the impact of TNF-NAb on brain inflammation in this model was at the level of recruitment of iMo into the brains of MCMV-infected animals and not secondary to activation of MNCs that infiltrated the brain.

Decreased frequency of $Ly6C^{hi}$ $CCR2^+$ inflammatory Mo in peripheral blood of TNF-NAb-treated mice. The decreased frequencies of nc-Mo, iMo, and lymphoid subsets observed in the brains of MCMV-infected mice treated with TNF-NAbs could be explained by decreased frequencies of these subsets of MNCs in peripheral blood, resulting in decreased recruitment to the brain. To address this possibility, we analyzed the frequencies of MNCs in peripheral blood of uninfected and MCMV-infected animals treated with TNF-NAbs or IC. In our analysis of $CD45^+$ MNCs that also expressed Ly6C

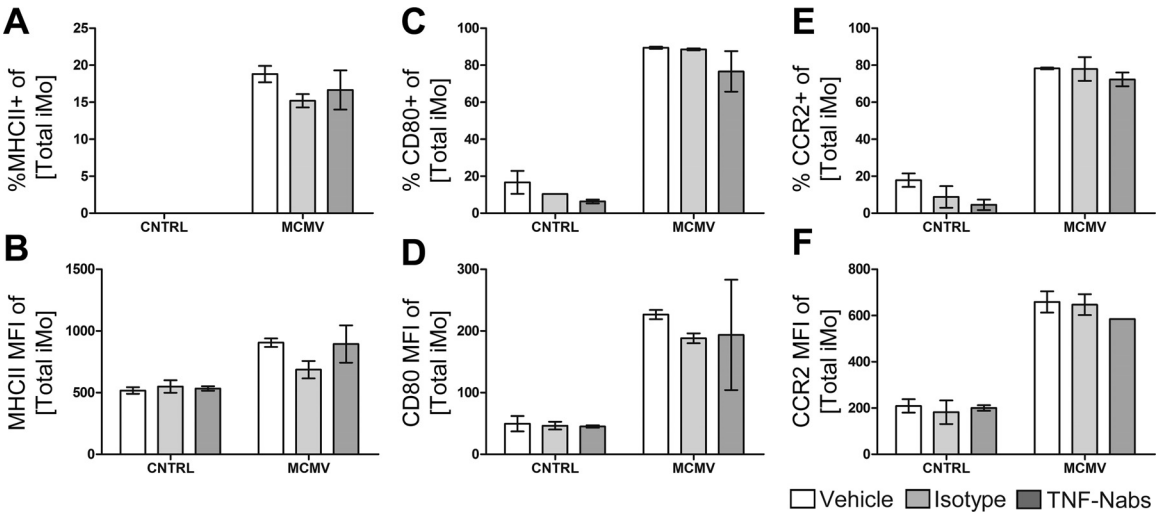

FIG 7 iMo that infiltrate the brains of MCMV-infected mice remain activated following TNF-NAb treatment. (A, C, and E) Frequencies of iMo gated as total live (CD45$^+$→CD11b$^+$ Ly6C$^+$→CD11b$^+$ Ly6C^{hi}) cells that expressed MHC-II (A), CD80 (C), and CCR2 (E) that were isolated from the brains of uninfected and MCMV-infected mice, untreated or treated with isotype control or TNF-NAbs. (B, D, and F) Quantification of expression of MHC-II (B), CD80 (D), and CCR2 (F) as MFI in iMo isolated from uninfected and MCMV-infected mice that were untreated or treated with isotype control or TNF-NAbs. The graphed data represent 2 or 3 replicates per group, with 4 mice pooled/replicate. The *P* values were calculated using two-way ANOVA with Bonferroni posttest correction.

and CD11b, we identified four MNC subsets in the blood of newborn mice: (i) nc-Mo, (ii) iMo, (iii) lymphoid cells, and (iv) CD45$^+$ cells that did not express CD11b or Ly6C (Fig. 8A). On day 8 post-MCMV infection (PND 8), the frequency of the Ly6C-expressing cells increased ~2.5-fold compared to uninfected mice, demonstrating a robust systemic response to infection (Fig. 8A). Concomitantly, the frequency of the CD11b$^-$ Ly6C$^-$ subset decreased ~3-fold compared to that in uninfected mice (Fig. 8A and data not shown). Compared to the respective frequencies in uninfected mice, the frequencies of nc-Mo, lymphoid cells, and iMo all increased significantly, confirming MCMV-induced activation of the myeloid and lymphoid components of the immune response in infected newborn mice (Fig. 8B). Following treatment of the MCMV-infected mice with TNF-NAbs or IC, the frequency of the nc-Mo subset was unchanged compared to that in untreated mice (Fig. 8B). While the frequency of the lymphoid subset in TNF-NAb-treated mice appeared to be decreased relative to that in untreated mice, it did not differ statistically from the frequency observed in IC-treated mice (Fig. 8B). In contrast, treatment with the TNF-NAbs resulted in a decrease in the frequency of iMo by more than 50% relative to infected untreated mice and IC-treated mice (Fig. 8A and B). This result suggested that TNF-NAbs preferentially impacted the iMo subset within peripheral blood. The frequency of cells that expressed the chemokine receptor CCR2 was then determined, as the presence of Ly6C^{hi} CCR2$^+$ monocytes has been associated with inflammation in the periphery, as well as within the CNS (67, 69, 75, 76). Interestingly, nearly all Ly6C^{hi} monocytes expressed CCR2, while virtually none of the Ly6C^{int} monocytes expressed the chemokine receptor (Fig. 8C and D). The frequency of Ly6C^{int} CCR2$^-$ monocytes (nc-Mo) remained unchanged by TNF-NAb treatment (Fig. 8C and D). Following treatment with TNF-NAbs, the frequency of Ly6C^{hi} CCR2$^+$ monocytes in MCMV-infected mice decreased significantly relative to untreated mice (Fig. 8D). In mice that were treated with IC, we observed a minimal but significant decrease in the frequency of this subset compared to untreated mice, suggesting that some of the *in vivo* effects of TNF-NAbs were nonspecific (Fig. 8D). Together, these data indicated that treatment with TNF-NAbs preferentially decreased the frequency of iMo in the peripheral blood of MCMV-infected mice and suggested that the reduced recruitment of iMo into the brain in this model of virus-induced inflammation was secondary to TNF-NAb effects on iMo in peripheral blood.

Neutralization of TNF-α correlates with decreased frequency of activated microglia in the brains of MCMV-infected neonatal mice. In addition to infiltrating

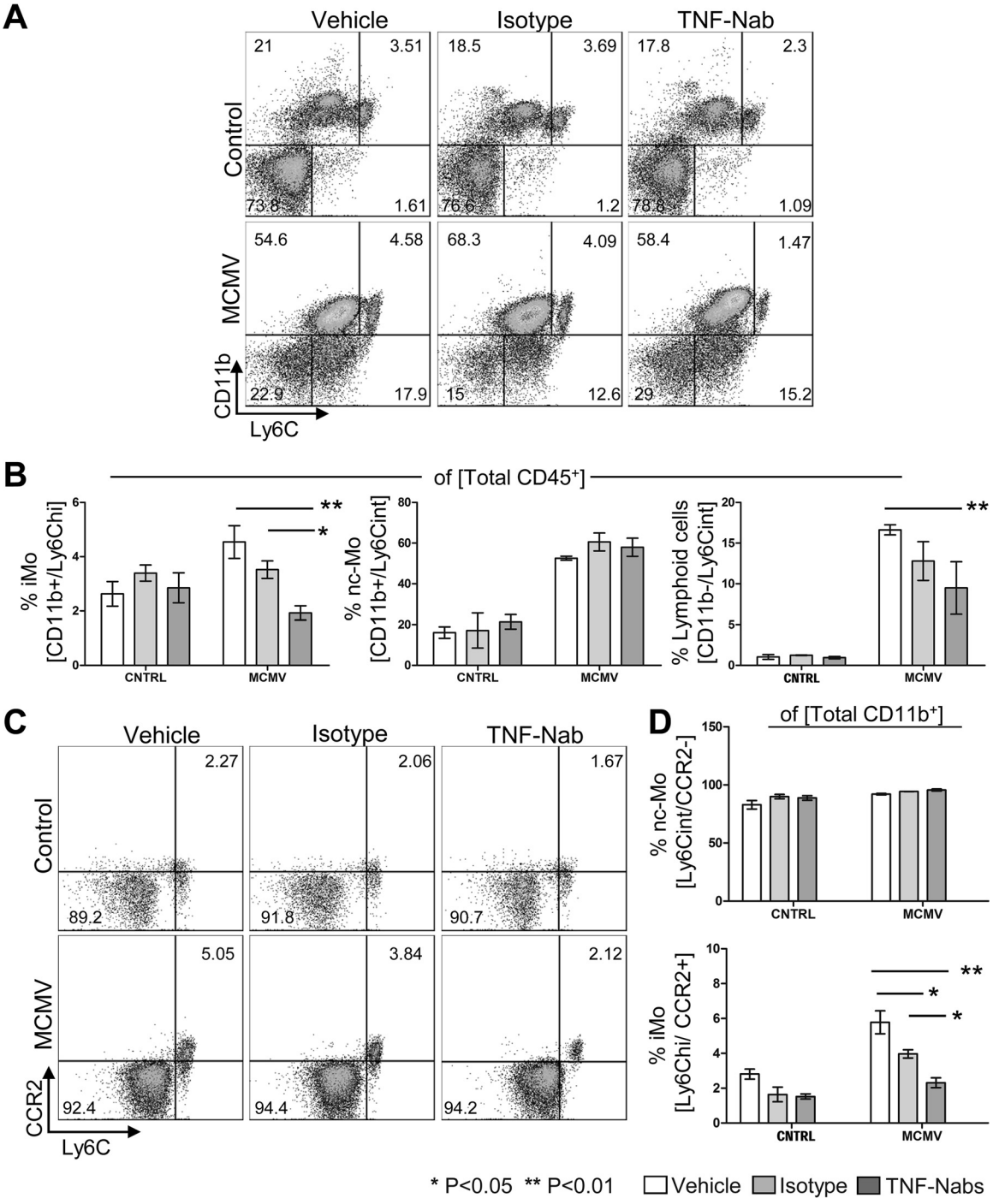

FIG 8 TNF-NAb treatment decreases the frequency of inflammatory monocytes (CD11b$^+$ Ly6C^{hi} CCR2$^+$) but not that of nonclassical monocytes or lymphocytes in blood of MCMV-infected newborn mice. (A and B) Representative flow cytometry dot plots showing peripheral blood subsets of uninfected or MCMV-infected mice that were left untreated or treated with TNF-NAbs or isotype control. (A) Expression of CD11b and Ly6C out of total (CD45$^+$) mononuclear cells. (B) corresponding quantification of iMo, nc-Mo, and lymphoid cells. (C) Expression of CCR2 and Ly6C within the myeloid compartment containing nc-Mo and iMo, gated on total CD45$^+$→SSC-A/CD11b$^+$ cells. (D) Corresponding quantification. The numbers within the dot plot quadrants are representative percentages of the corresponding MNC subsets. The data are shown as means ± SEM; $n = 2$ or 3 replicates, with 4 mice pooled per replicate. The P values were calculated using two-way ANOVA, with Bonferroni posttests.

activated iMo, the activation of microglia has also been linked to increased CNS pathology in neurodegenerative, autoimmune, and infectious diseases (72, 77). In MCMV infection of the developing CNS, we have described robust MCMV-induced microglial activation indicated by upregulation of MHC-II molecules (28, 29). Consistent

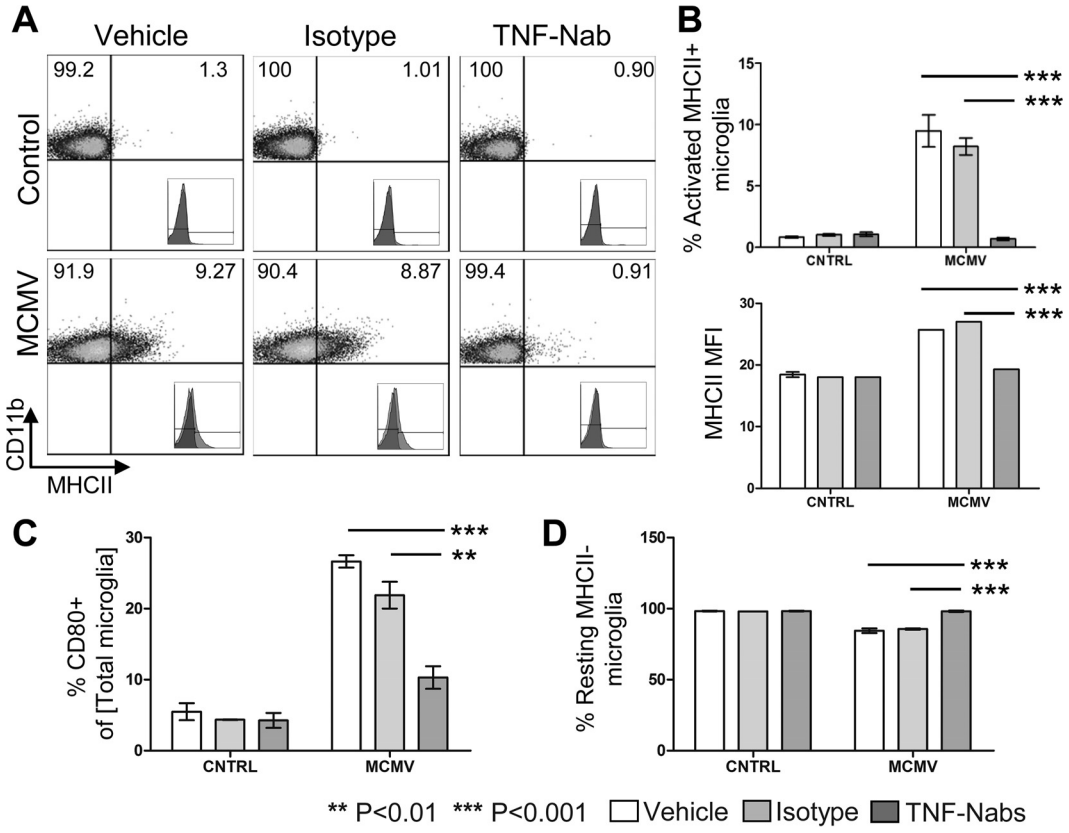

FIG 9 Decreased frequency of activated resident microglia in the brains of TNF-NAb-treated MCMV-infected mice. (A) Representative flow cytometry dot plots showing microglial cells, gated ($CD45^+$ $CD11b^+$ $Ly6C^-$) and defined, respectively, as activated (MHC-II expression [$MHC\text{-}II^+$]) or resting microglia. Representative cell percentages are shown within each quadrant. The histograms (insets) show $MHC\text{-}II^+$ cell expression versus MHC-II antibody isotype controls. The cells analyzed were isolated from the brains of uninfected or MCMV-infected mice that were left untreated or treated with isotype or the TNF-NAbs. (B and C) Quantification of the percentages of activated (]$MHC\text{-}II^+$) microglia and MHC-II MFI levels (B) and percentages of $CD80^+$ activated microglia (C). (D) Resting microglial cells, defined as $MHC\text{-}II^-$, gated as described for panel A. The data represent 2 or 3 replicates per group, with 4 mice pooled/replicate. The *P* values were calculated using two-way ANOVA, with Bonferroni posttests.

with previous findings, MCMV infection induced an ~7-fold increase in the frequency of $MHC\text{-}II^+$ microglial cells ($Ly6C^-$ $CD11b^+$ $CD45^{low}$) compared to that in uninfected mice, whereas the proportion of resting microglia ($MHC\text{-}II^-$) decreased in MCMV-infected mice compared to uninfected mice (Fig. 9A, B, and D). Similarly, the frequency of $CD80^+$ microglial cells increased by nearly 4-fold following MCMV infection compared to uninfected mice (Fig. 9C). Following treatment with TNF-NAb, the frequency of $MHC\text{-}II^+$ microglial cells decreased to levels that were similar to the average frequency observed in uninfected mice, and the fraction of resting $MHC\text{-}II^-$ microglia was similar to that observed in uninfected animals (Fig. 9B and D). The average MHC-II MFI value of activated microglia isolated from infected TNF-NAb-treated mice decreased significantly compared to the average MFI levels observed in untreated, infected, or IC-treated mice (Fig. 9B). Together, these results indicated that TNF-NAb treatment resulted in a decrease of activated microglia, further supporting our initial hypothesis that TNF-α is a major inflammatory mediator in the CNS of MCMV-infected neonatal mice.

iMo expresses the highest levels of TNF-α among all MNC subsets isolated from brain and blood. We next determined which specific MNC subset isolated from the brains or blood of PND 8 MCMV-infected mice expressed *TNF-α* and thus could be targeted by the *TNF-α*-neutralizing activities of TNF-NAb and/or possibly by effector functions, such as antibody-dependent cell-mediated cytotoxicity (ADCC) directed against cells expressing membrane-bound *TNF-α* (78, 79). MNC isolates from brain or

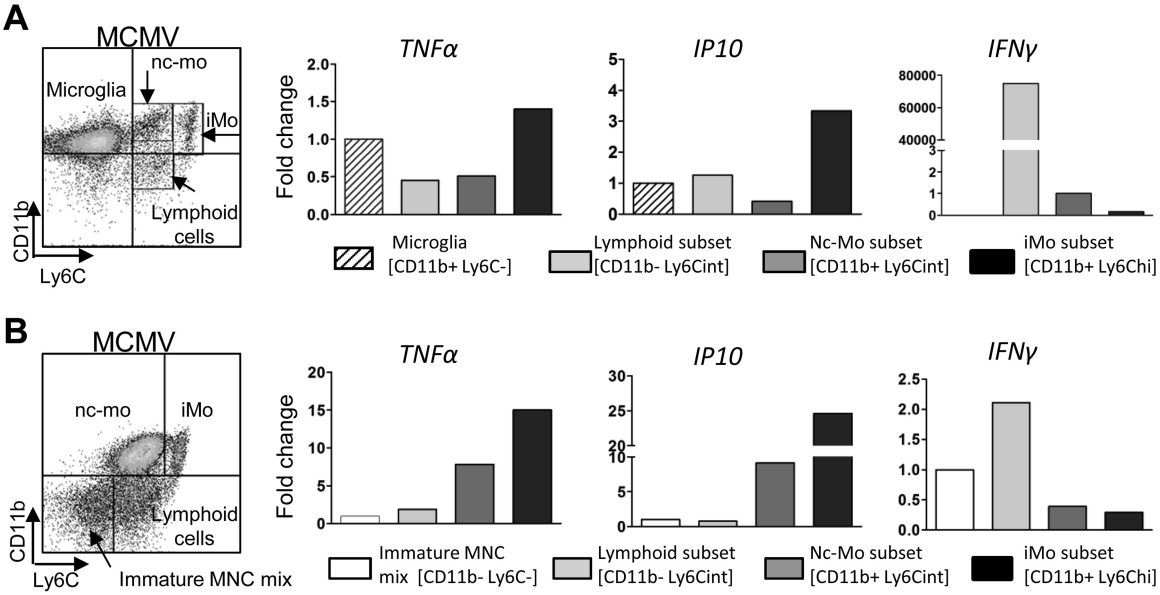

FIG 10 Proinflammatory molecules are differentially expressed in mononuclear cell subsets isolated from peripheral blood or brains of MCMV-infected newborn mice. Shown are representative flow cytometry dot plots of brain-derived (A) and blood-derived (B) mononuclear cell subsets that differentially expressed Ly6C and/or CD11b that were gated on total ($CD45^+$) mononuclear cells. The different cell populations were sorted according to their expression of the surface markers Ly6C and CD11b. The graphs show the relative expression of *TNF-α*, *IP10*, or *IFN-γ* in subsets derived from brain (A) or blood (B). (A) The microglial subset was used to set the comparative reference value, with the exception of the *IFN-γ* expression, for which the response of the nc-Mo subset was used because *IFN-γ* expression was not observed in the microglial subset. (B The immature MNC mixture was set as the comparative reference sample. In all assays, the housekeeping gene *β-actin* was used as an internal reference control.

blood were sorted by fluorescence-activated cell sorter (FACS) according to their expression of CD45, CD11b, and Ly6C, and the expression of *TNF-α* RNA was quantified (Fig. 10). Relative gene expression was quantified by comparison of *TNF-α* expression levels in microglial cells as a reference for MNCs isolated from the brains of infected mice. Among microglial, lymphoid, nc-Mo, or iMo MNC subsets from the brain, the highest level of *TNF-α* expression was seen in the iMo (Fig. 10A). This result indicated that among the MNCs present in the brains of MCMV-infected newborn mice, iMo and microglial cells represented the primary sources of proinflammatory *TNF-α*. In MNC subsets sorted from blood, the relative expression of *TNF-α* was again highest in iMo (Fig. 10B). Finally, blood- and brain-derived lymphoid cells expressed low levels of *TNF-α* (Fig. 10A and B). To validate the correct biological assignment of the different cell subsets that were isolated by sorting, we analyzed the expression of *IP10*, encoding a T-cell chemoattractant that has been reported to be expressed primarily by activated monocytes, macrophages, or dendritic cells, and *IFN-γ*, encoding another cytokine highly associated with inflammation and typically expressed by effector NK and CD8 T cells. The iMo subsets in both brain and blood MNCs expressed high levels of *IP10* (Fig. 10A and B). In contrast, these cell subsets expressed the lowest levels of *IFN-γ* (Fig. 10A and B). These results suggest that among MNCs present at this time, the brain and blood iMo were activated by proinflammatory monocytes and produced the highest levels *TNF-α* and other proinflammatory marker genes, such as *IP10*. The microglial subset expressed *IP10*, consistent with the function of activated microglia in the recruitment of effector leukocytes (Fig. 10A) (80). In contrast, *IFN-γ* expression was not detected in the microglial subset, and the level of expression of *IFN-γ* in nc-Mo was modest in comparison to the level of expression detected in lymphocytes present in the brain (Fig. 10A). Both brain- and blood-derived lymphoid subsets expressed low levels of *IP10* (Fig. 10A and B). Together, these data raise the possibility that TNF-NAbs could impact CNS inflammation, not only by limiting recruitment of iMo to the brain and modulating microglial activation, but also by either neutralizing soluble *TNF-α* in the brain or targeting *TNF-α*-expressing cells in the MCMV-infected brain.

DISCUSSION

Animal models have provided insight into the proposed disease mechanisms of congenital HCMV infection, but each model has limitations, and none completely recapitulates human infection (3, 4, 9, 81–84). To address the shortcomings of previously described small-animal models, particularly those that relied on direct intracranial inoculation of virus, we developed a murine model of congenital HCMV infection utilizing peripheral (intraperitoneal) inoculation of newborn mice with nonlethal doses of MCMV (26). The model was developed in newborn mice because the neurodevelopmental status of mice at this age has been shown to be nearly equivalent to that of a late second trimester human fetus (85). Thus, the immaturity of the CNS in newborn mice has enabled us to experimentally explore the impact of infection and virus-induced inflammation of the brain during a dynamic period of neurodevelopment. In addition, the model recapitulates the hematogenous route of CNS infection following intrauterine HCMV infection of the human fetus. The replication of MCMV in brains of infected mice resulted in a robust inflammatory response and a number of neurodevelopmental abnormalities ranging from delayed expression of developmentally regulated genes to altered cellular positioning in the cerebellum (26, 29). Utilizing this mouse model, we have shown that treatment of infected mice with prednisolone, a relatively nonspecific anti-inflammatory agent, normalized deficits in cerebellar development associated with MCMV infection (29). In addition, prednisolone treatment decreased both expression of inflammatory mediators in the cerebellum and the frequency of $CD45^+$ $CD11b^+$ mononuclear cells in the brains of infected mice. Because the level of virus replication in the CNS was not altered by this short-term corticosteroid treatment, these results argued that virus-induced inflammatory responses, and not direct viral cytopathology, were responsible for the developmental abnormalities in the CNS observed in infected mice (29). Although studies of other viral infections have documented the contribution of inflammatory responses to tissue pathology, our findings were novel in that virus-induced inflammation was associated with focal, nonfatal viral encephalitis that resulted in global and symmetric abnormalities in CNS development without significant destruction of brain parenchyma. Together, our findings argue that a balance between control of viral replication and the development of immunopathology must be achieved to limit disease in the developing brain (28, 29).

In the current study, we attempted to further define specific inflammatory mediators that contributed to the altered CNS development induced by the virus. Our studies demonstrated that treatment with TNF-NAbs efficiently decreased CNS inflammation and limited deficits in cerebellar development in MCMV-infected neonatal mice, clearly implicating this proinflammatory molecule in the pathogenesis of the infection. Although TNF-α has pleiotropic effects *in vivo*, our findings argued that treatment with TNF-NAb decreased CNS inflammation by decreasing the frequency of activated $CD45^+$ $Ly6C^{hi}$ $CD11b^+$ $CCR2^+$ iMo in the brain. Furthermore, our data also suggested that TNF-NAb decreased infiltration of blood iMo into the brains of infected mice by reducing their numbers in peripheral blood and not by directly decreasing the activation state of iMo in the brains of infected animals. Findings from previous studies in WNV encephalitis models have also argued that infiltration of iMo into the brains of WNV-infected mice was dependent on CCR2/CCL2 monocytosis in peripheral blood and not secondary to CCR2/CCL2-driven recruitment of iMo to the infected brain (73, 86). It is also of interest that MCMV infection of adult mice results in Myd88-dependent mobilization and activation of monocytes in the bone marrow and that, in contrast to type I IFNs, IL-6, or IL-1, TNF-α appeared to potentially have a direct role in mobilization and activation of monocytes from the bone marrow (87). Although our results are consistent with TNF-NAb inhibition of mobilization and activation of monocytes from the bone marrow and decreased blood and brain iMo, it is important to note that these observations were made in adult mice, in which the bone marrow is a major source of myeloid mononuclear cells.

TNF-α has been shown to function in the recruitment of peripheral monocytes to

sites of injury in experimental models of inflammatory disease in different organ systems, including the CNS. Studies in a murine model of *Listeria monocytogenes* have demonstrated that peripheral infection and innate responses, including IFN-γ and TNF-α production, were associated with an upregulation of proinflammatory genes and the induction of adhesion molecules and chemokines in the CNS (88, 89). In addition, in some models of virus infection of the brain by a systemic route, monocytes expressing Ly6C$^+$ infiltrated the brain prior to CNS infection, suggesting that peripheral responses to infection contributed to recruitment of proinflammatory monocytes into the brain (88). Recruitment of proinflammatory monocytes to the CNS and other tissues following infection has been argued to be dependent on MCP-1 and MCP-3 (90, 91). As MCP-1 is a high-affinity ligand of CCR2, our findings were consistent with these earlier studies that had described MCP-1-mediated recruitment of activated CCR2$^+$ peripheral blood MNCs into the CNS. However, it should be noted that in more recent studies, the recruitment of inflammatory monocytes from the blood to tissue has been shown to be independent of CCR2 expression by iMo and that MCP-1 appears to function primarily by increasing mobilization of monocytes from the bone marrow (89). Thus, in our study, the depletion of blood iMo by TNF-NAb treatment appears to be the most likely mechanism for the decrease of iMo in the brains of MCMV-infected mice, but we cannot exclude the possibility that some of the decrease was secondary to the decrease in the frequency of proinflammatory resident cells of the brain, including microglia. Finally, it is important to note that although treatment with TNF-NAb dramatically reduced the frequency of activated microglia in the brains of infected animals to levels measured in mock-infected animals, iMo that infiltrated the brains of TNF-NAb-treated animals continued to express activation markers, providing evidence that resident cells of the infected brain are not the sole determinants of inflammation in the brain in infected animals.

Studies in other small-animal models of virus-induced CNS disease associated with inflammation have described the importance of infiltrating monocytes in the induction of disease (38, 74, 92). Furthermore, limiting the infiltration of peripheral blood monocytes, including the Ly6C^{hi} CCR2$^+$ subset, into the CNS resulted in improved disease outcomes in murine models of amyotrophic lateral sclerosis (ALS), demyelinating diseases associated with virus infection, experimental autoimmune encephalitis (EAE), and CNS ischemia (67, 69, 93, 94). Early studies described a proinflammatory phenotype of CNS-infiltrating monocytes (CD45^{hi}), often together with the expression of MHC-II and/or other activation markers (95). More recently, proinflammatory monocytes infiltrating the CNS have been defined by the expression of CCR2 and Ly6C, and in some cases together with activation markers (67, 96). These markers define M1 monocytes, thought to have a major role in the early response to tissue injury/infection and associated with immunopathology (96).

The role of iMo in resistance to viral infection of the brain has been most extensively studied in recent years in the mouse of model of WNV encephalitis (97). iMo are thought to play a critical role in resistance to lethal encephalitis in this model, as depletion of iMo through the use of transgenic mice, chemical treatments, or biologics, such as anti-TNF monoclonal antibodies (MAbs), has resulted in increased levels of virus replication in the brain and decreased survival of WNV-infected mice. In contrast to these findings, other authors have argued that a reduction in the infiltration of Ly6C^{hi} mononuclear cell infiltration into the CNS of WNV-infected mice prolonged survival of the infection, an effect that at least one study suggested was independent of the level of virus replication (98). Validation of these initial findings was reported in a study from the same group of investigators, who demonstrated that depletion of inflammatory monocytes (CD45$^+$ CD11b$^+$ Ly6C^{hi}) with microparticles improved the survival and outcome of WNV-infected mice, an outcome that was associated with a decrease in the brain infiltration of iMo (99). Similar to our findings, the impact of the microparticle treatment leading to decreased CNS infiltration of iMo appeared to be secondary to depletion of these cells in the peripheral blood and not loss of iMo that had entered the brain (99). Our findings in this model of CMV infection of the developing brain are

consistent with results from this study of WNV infection of the CNS and argued that decreased infiltration of iMo into the brain limited the neurodevelopmental abnormalities in MCMV-infected mice. Although clearance of virus from the brain by virus-specific $CD8^+$ T lymphocytes is critical to both model systems, several features of our system utilizing MCMV are notably different than WNV models of CNS infection and could account for some of the discordance between findings in WNV encephalitis in adult mice and MCMV focal CNS infection in newborn mice (28, 100, 101). These differences include (i) the nature of the encephalitis induced by the two viruses; (ii) the developmental status of the infected animal; and importantly, (ii) the limited neurotropism of MCMV compared to WNV. In contrast to direct virus-induced neurological damage postulated in WNV encephalitis, our findings in this murine model of CMV brain infection demonstrated that the interface between early effector functions in virus-induced inflammation and the developing brain likely contributed to the neurological damage that resulted from the infection.

In this model of CMV infection of the developing brain, robust activation of microglia and infiltration of $Ly6C^{int}$ $CD11b^{low/-}$ cells into the CNS was observed in MCMV-infected mice (Fig. 6E and 9). The $Ly6C^{int}$ $CD11b^{low/-}$ population was comprised of about 50% NK cells, a finding that was consistent with their production of high levels of IFN-γ (Fig. 10A). Thus, in light of recent studies suggesting a role for NK cells in murine models of demyelinating diseases, such as EAE, and virus-induced demyelination, we cannot exclude the potential contribution of infiltrating NK cells to the inflammation in the brains of MCMV-infected mice (102, 103). Similarly, NK cells have been proposed to provide protective antiviral activities in models of viral encephalitis, including coronavirus encephalitis, although the precise role of NK cells in WNV encephalitis remains less well understood (104, 105). However, it is important to note that NK cell function in neonatal mice is developmentally immature and cannot be compared to results from studies in adult mice (106). In contrast, activated microglia have been suggested to contribute immunopathological responses to chronic viral infections of the CNS, such as HIV, as well as to provide early antiviral responses during acute viral encephalitis associated with both flaviviruses and herpes simplex virus (107–109). However, similar to limitations in our study, the previous studies were often carried out in the presence of peripheral inflammatory responses, and thus, the precise role of microglia in the mechanisms of CNS disease cannot be rigorously assigned. Regardless of the role of microglia or NK cells, neutralization of TNF-α resulted in the decreased transcription of *IL-1*β, *IFN-*β, and *IFN-*γ (in addition to *TNF-*α) in the cerebellum, as well as decreased expression of proinflammatory chemokines. Collectively, our findings demonstrated that TNF-NAb treatment decreased the frequency of activated microglia and infiltration of both iMo and NK cells into the brains of MCMV-infected mice and thus argued that TNF-α was a key initiator of inflammation in the brains of MCMV-infected mice.

In summary, our findings demonstrated that treatment of MCMV-infected neonatal mice with TNF-NAbs dramatically decreased CNS inflammation and resulted in normalization of neurodevelopmental markers. TNF-NAb treatment did not significantly alter the levels of virus replication in the CNS, providing further evidence that virus-induced inflammation, and not the direct effects of virus infection, was responsible for the developmental abnormalities in the brains of MCMV-infected mice. Specific mechanisms of action of TNF-α-induced inflammation in the CNS remain incompletely defined, but a major effect of TNF-NAb treatment was the decreased infiltration of activated $Ly6C^{hi}$ $CCR2^+$ iMo into the brains of infected mice secondary to the loss of iMo from the peripheral blood. Thus, if a similar TNF-α-regulated pathway represents a mechanism of damage and neurodevelopmental deficits found in infants following intrauterine infection with HCMV, then interventions modulating the trafficking of iMo from the peripheral blood into the CNS could offer a therapeutic approach for prevention of neurologic sequelae characteristic of this intrauterine infection.

MATERIALS AND METHODS

Ethics statement. The University of Alabama—Birmingham (UAB) Institutional Animal Care and Use Committee (IACUC) guidelines were followed for all animal experiments and breeding. These guidelines are in strict compliance with the NIH (Office of Laboratory Animal Welfare [OLAW] assurance number A32555-01) guidelines. Animals were euthanized with carbon dioxide under regulated flow. Following carbon dioxide administration, cervical dislocation was implemented to ensure the animals were completely euthanized prior to carrying out experimental protocols, according to the UAB Animal Resource Program (ARP) guidelines. An approved protocol was obtained from the IACUC for all experiments. All the experiments done at the University of Rijeka were in accordance with the University of Rijeka, Croatia, animal use and care policies and the guidelines of the animal experimentation law (SR 455.163; Töten von Versuchstieren [TVV]) of the Swiss Federal Government.

MCMV infection and TNF-NAb treatment. BALB/cJ mice were purchased from the Jackson Laboratory (Bar Harbor, ME). Mouse pups were infected with 500 PFU of MCMV Smith (ATCC VR-1399) in 50 μl of sterile 1× phosphate-buffered saline (PBS). Virus was delivered by intraperitoneal (i.p.) injection of newborn BALB/c mice no more than 12 h following birth, as previously described (26, 29). On PND 4 to 7, pups were treated by i.p. injection with neutralizing rat monoclonal antibodies to TNF-α (kindly provided by David Shealy, Janssen Pharmaceuticals, Titusville, NJ) at 500 μg/mouse/day. TNF-NAbs were diluted in 1× PBS. As a control, uninfected and MCMV-infected animals were given i.p. injections with 500 μg/mouse/day of rat IgG2a (isotype control) antibodies, also diluted in 1× PBS. Control and MCMV-infected mice that were not treated with either TNF-NAbs or isotype antibodies received a vehicle injection of sterile 1× PBS alone. For all treatments, a volume of 50 μl was administered. On PND 8, between 16 and 18 h post-final treatment, the mice were sacrificed and perfused with ice-cold PBS, and organs were harvested. Once isolated, the organs were prepared for the appropriate assay. Infection of newborn mouse pups was confirmed by quantitative real-time PCR measurement of MCMV genome equivalents, as previously described, using the StepOne Plus system from Applied Biosystems (Carlsbad, CA) (29).

Cytokine measurements. For analysis of cytokine/chemokine levels in the cerebellum, 3 cerebella were pooled, weighed, and homogenized, utilizing a Dounce homogenizer, on ice in 600 μl of 1× PBS, 0.1% Triton X-100 plus a protease/phosphatase inhibitor cocktail with EDTA (Thermo Scientific, Waltham, MA). The homogenates were then sonicated 3 times for 10 s each time with a 10-s incubation on ice between sonications. Samples were then centrifuged at 14,000 rpm for 30 min at 4°C. Following centrifugation, the samples were aliquoted and stored at −80°C until use. Cerebellar cytokine/chemokine levels were determined by Milliplex map multiplex assay (Millipore, Billerica, MA) according to the manufacturer's instructions. Cytokine levels in the sera of control and MCMV-infected mice were determined by Bioplex cytokine assay (Bio-Rad, Hercules, CA) using the protocol provided by the manufacturer.

Immunofluorescence, immunohistochemistry, and cerebellar morphometry. Immunofluorescent staining of BrdU and Ki67 was performed by previously published methods (29). Briefly, mice were injected on PND 8 with 50 μg/g of body weight of BrdU (Sigma-Aldrich) 6 h prior to sacrifice. The mice were perfused with PBS, and their brains were fixed in 4% paraformaldehyde (PFA) overnight, cryoprotected in 30% sucrose-PBS, and embedded in Tissue Tek OCT compound (Andwin Scientific); 8-μm sagittal sections were cut using a Leica cryostat and then dried for 4 h at room temperature (RT), rehydrated in 1× PBS, and used for immunofluorescence assays. The sections were blocked for 1 h at RT, followed by a 2 N HCl acid wash. The sections were then buffered in 0.1 M borate buffer, washed, and incubated in primary antibody overnight at RT. The following day, the sections were washed and incubated in secondary antibody for 2 h at RT in the dark. The sections were again washed and incubated with Hoescht stain (in 1× PBS) for 15 min at RT in the dark and then mounted using Vectashield fluorescent mounting medium (Vector Laboratories).

Staining for Iba-1 and CD169 was as follows. Sections were blocked in 1× PBS, 0.05% Triton X-100, 20% normal goat serum, 5% bovine serum albumin (BSA) for 2 h at RT. The sections were then washed in 1× PBS, 0.01% Triton X-100 and stained with primary antibodies (in blocking buffer) at RT for 2 h. Subsequently, the sections were washed 3 times for 5 min/wash with 1× PBS, 0.01% Triton X-100 and then incubated for 2 h at RT in the dark with secondary antibodies (in blocking buffer). After incubation with secondary antibodies, the sections were washed 5 times for 5 min/wash with 1× PBS, 0.01% Triton X-100 and incubated with Hoescht stain (in 1× PBS) for 15 min at RT. Following nuclear staining with Hoescht stain, the sections were washed 3 times for 5 min/wash with 1× PBS and then postfixed with 4% PFA for 15 min at RT. The sections were washed 5 times for 2 min/wash following postfixing and then mounted with Vectashield.

The primary antibodies used were as follows: rat anti-BrdU (1:50; ab6326; Abcam), rabbit anti-Ki67 (1:200; ab66155; Abcam), rabbit anti-Iba-1 (1:200; Wako, Japan), and rat anti-CD169 (1:100; BioLegend). The secondary antibodies used were goat anti-rabbit tetramethyl rhodamine isocyanate (TRITC)/ fluorescein isothiocyanate (FITC) and goat anti-rat TRITC/FITC (1:150; Southern Biotech, Birmingham, AL). Hoescht stain (1:1,000; Thermo Scientific) was used as a nuclear marker. Images of stained sections were collected with an Olympus (Center Valley, PA) FluoView FV1000 confocal microscope at either ×40 magnification or ×60 magnification, as indicated. For all images, the imaging medium used was Olympus oil, and all images were captured using FluoView software. All morphometric measurements and cell counts were done as previously described and analyzed using Image J software according to our previous protocol (29, 110).

Quantitative real-time reverse transcription-PCR. TRIzol reagent (Roche Applied Science, Indianapolis, IN) was used to isolate total RNA from the cerebellum, as described previously (29). The Invitrogen Superscript III First Strand synthesis kit was used to synthesize cDNA, and real-time

reverse transcription-PCR was performed according to our previous protocol. TaqMan assay mixtures from Applied Biosystems (Life Technologies, Carlsbad, CA) were used for *TNF-α* (Mm99999068), *MCP-1* (Mm00656886), *IFN-β* (Mm00439552), *STAT1* (Mm00439518), *IFN-γ* (Mm99999071), *IFIT1* (Mm00515153), *IL-1β* (Mm00434228), *IRF7* (Mm00516793), *gli1* (Mm00494645), *N-myc* (Mm00476449), *Tiam1* (Mm01170430), *CDK5* (Mm00432437), and *GABRA6* (Mm01227754). The Applied Biosystems StepOne Plus real-time PCR machine was used to analyze gene transcription. Fold changes for all experimental groups were normalized to control values (termed the relative fold change).

Virus genome copy quantitation. The liver was collected from each animal, as well as a small piece of spleen, brain, and cerebellum (~50 mg) randomly collected for the analysis of viral genome copies by quantitative PCR (qPCR), as we have described in previous publications (26, 29). The results were expressed as log genome copies per milligram of tissue.

Flow cytometry, acquisition, and sorting. For all flow cytometry experiments, tissue or blood was pooled from 3 or 4 animals, and each experiment was repeated a minimum of 3 times. Following CO_2 euthanasia, about 150 to 200 μl of whole blood was obtained from the axillary arteries and by cardiac puncture. Then, the brain was dissected from ice-cold-PBS-perfused mice. Following dissection, the organs were dissociated in a Gentle-Macs (Milteny, Auburn, CA) apparatus, and the cell suspensions were cleared through 40-μm (blood) or 70-μm (brain) strainers before being subjected to centrifugation at 600 × *g* for 30 min over a 30%-70% discontinuous Percoll gradient for blood or 690 × *g* for 20 min over a 37.5% continuous Percoll gradient for brain. The mononuclear cell pellet (brain) or the band formed at the 30%-70% interphase (blood) were collected, washed once in RPMI medium and in FACS buffer before incubation for 30 min on ice with Fc-block (1:100; CD16/CD32; BioLegend, San Diego, CA). Subsequently, the cell suspensions were pelleted, resuspended in the appropriate staining cocktail, and incubated for 30 min at 4°C. Following two washes in Dulbecco's phosphate-buffered saline (DPBS), the cells were incubated for another 20 min at 4°C, with the fixable viability dye eFluor 450 (eBiosiences, San Jose, CA) to allow LIVE/DEAD cell discrimination. The cells were subsequently washed twice in DPBS before being fixed in 2% PFA for 15 min at 4°C. Following 2 washes in PBS, the cells were resuspended in FACS buffer, and flow cytometry acquisition was conducted on a FACSVerse (BD Biosciences, San Jose, CA.) analyzer. The data were analyzed using FlowJo V10.0.8r1. For cell sorting, we followed the same procedure, except that the cells were not fixed in PFA before being subjected to 4-way cell sorting in a BD FACSAria instrument (BD Biosciences, San Jose, CA) at the UAB Comprehensive Flow Cytometry Core (NIH P30 AR048311, Rheumatic Disease Core Center [RDCC], NIH P30 AI27667, Center for AIDS Research [CFAR]). The sorted cells were collected in RPMI (10% fetal bovine serum [FBS]) before being lysed in GTC RNA lysis buffer (Omega Bio-tek, Norcross, GA). The different antibodies, isotype controls, and corresponding fluorochromes used in this work were as follows: FITC-anti-CD80 (clone 16-10A1; eBiosciences), FITC-anti-CD45 (clone 30-F11; eBiosciences), phycoerythrin (PE)-conjugated anti-CCR2 (475301; RD Systems), PE-conjugated anti-CD3e chain (clone 145-2c11; BD Pharmingen), peridinin chlorophyll protein (PerCP)-Cy5.5-conjugated anti-Ly6C (clone HK1.4; eBiosciences), PE-Cy7-conjugated IA/IE (i.e., MHC-II subclasses H2A and H2E) (clone M5/114.15.2; BioLegend), allophycocyanin (APC)-CD11b (clone M1/70; eBiosciences), AF660-conjugated anti-NKp46 (clone 29A1.4; eBiosciences), APC-Cy7 anti-CD11b (M1/70; BD Biosciences), BV510-conjugated anti-CD45 (clone 30-F11; BD Biosciences), TruStainfc anti-CD16/CD32 (clone 93; BioLegend), and the fixable viability dye eFluor V450 (eBiosciences).

Statistics. For all comparisons between mean values from control and infected animals, a two-tailed *t* test was used to determine statistical significance. Two-way analysis of variance (ANOVA), followed by Bonferroni's posttest, was used to determine significance across treatment groups. Median viral genome copy numbers were analyzed using a Kruskal-Wallis test of medians with Dunn posttest correction. All statistical analysis was carried out using Prism 5 software (GraphPad, San Diego, CA).

ACKNOWLEDGMENTS

We thank David Shealy (Janssen Pharmaceuticals, Malvern, PA) for generously providing the neutralizing antibody to TNF-α. We also thank Oleg Butovsky (Harvard University) for helpful discussions and for providing the CD169 antibody with optimized protocols for tissue staining.

REFERENCES

1. Boppana S, Britt WJ. 2013. Synopsis of clinical aspects of human cytomegalovirus disease, p 1–25. *In* Reddehase M (ed), Cytomegaloviruses: from molecular pathogenesis to intervention, vol 2. Caister Academic Press, Norfolk, United Kingdom.
2. van den Pol AN. 2006. Viral infections in the developing and mature brain. Trends Neurosci 29:398–406. https://doi.org/10.1016/j.tins.2006.06.002.
3. Tsutsui Y, Kosugi I, Kawasaki H, Arai Y, Han GP, Li L, Kaneta M. 2008. Roles of neural stem progenitor cells in cytomegalovirus infection of the brain in mouse models. Pathol Int 58:257–267. https://doi.org/10.1111/j.1440-1827.2008.02221.x.
4. Tsutsui Y, Kosugi I, Kawasaki H. 2005. Neuropathogenesis in cytomegalovirus infection: indication of the mechanisms using mouse models. Rev Med Virol 15:327–345. https://doi.org/10.1002/rmv.475.
5. Kosugi I, Shinmura Y, Kawasaki H, Arai Y, Li RY, Baba S, Tsutsui Y. 2000. Cytomegalovirus infection of the central nervous system stem cells from mouse embryo: a model for developmental brain disorders induced by cytomegalovirus. Laboratory Invest 80:1373–1383. https://doi.org/10.1038/labinvest.3780145.
6. Bale JF, Jr, Murph JR. 1997. Infections of the central nervous system in the newborn. Clin Perinatol 24:787–806.
7. Luo MH, Schwartz PH, Fortunato EA. 2008. Neonatal neural progenitor cells and their neuronal and glial cell derivatives are fully permissive for human cytomegalovirus infection. J Virol 82:9994–10007. https://doi.org/10.1128/JVI.00943-08.
8. Pan X, Li XJ, Liu XJ, Yuan H, Li JF, Duan YL, Ye HQ, Fu YR, Qiao GH, Wu CC, Yang B, Tian XH, Hu KH, Miao LF, Chen XL, Zheng J, Rayner S, Schwartz PH, Britt WJ, Xu J, Luo MH. 2013. Later passages of neural progenitor cells from

neonatal brain are more permissive for human cytomegalovirus infection. J Virol 87:10968–10979. https://doi.org/10.1128/JVI.01120-13.
9. Tarantal AF, Salamat MS, Britt WJ, Luciw PA, Hendrickx AG, Barry PA. 1998. Neuropathogenesis induced by rhesus cytomegalovirus in fetal rhesus monkeys (Macaca mulatta). J Infect Dis 177:446–450. https://doi.org/10.1086/514206.
10. Mutnal MB, Cheeran MC, Hu S, Lokensgard JR. 2011. Murine cytomegalovirus infection of neural stem cells alters neurogenesis in the developing brain. PLoS One 6:e16211. https://doi.org/10.1371/journal.pone.0016211.
11. Gabrielli L, Bonasoni MP, Lazzarotto T, Lega S, Santini D, Foschini MP, Guerra B, Baccolini F, Piccirilli G, Chiereghin A, Petrisli E, Gardini G, Lanari M, Landini MP. 2009. Histological findings in foetuses congenitally infected by cytomegalovirus. J Clin Virol 46(Suppl 4):S16–S21. https://doi.org/10.1016/j.jcv.2009.09.026.
12. Lanari M, Capretti MG, Lazzarotto T, Gabrielli L, Rizzollo S, Mostert M, Manzoni P. 2012. Neuroimaging in CMV congenital infected neonates: how and when. Early Hum Dev 88(Suppl 2):S3–S5. https://doi.org/10.1016/S0378-3782(12)70003-8.
13. Barkovich AJ, Lindan CE. 1994. Congenital cytomegalovirus infection of the brain: imaging analysis and embryologic considerations. Am J Neuroradiol 15:703–715.
14. de Vries LS, Gunardi H, Barth PG, Bok LA, Verboon-Maciolek MA, Groenendaal F. 2004. The spectrum of cranial ultrasound and magnetic resonance imaging abnormalities in congenital cytomegalovirus infection. Neuropediatrics 35:113–119. https://doi.org/10.1055/s-2004-815833.
15. Doneda C, Parazzini C, Righini A, Rustico M, Tassis B, Fabbri E, Arrigoni F, Consonni D, Triulzi F. 2010. Early cerebral lesions in cytomegalovirus infection: prenatal MR imaging. Radiology 255:613–621. https://doi.org/10.1148/radiol.10090749.
16. Sugita K, Ando M, Makino M, Takanashi J, Fujimoto N, Niimi H. 1991. Magnetic resonance imaging of the brain in congenital rubella virus and cytomegalovirus infections. Neuroradiology 33:239–242. https://doi.org/10.1007/BF00588225.
17. Picone O, Simon I, Benachi A, Brunelle F, Sonigo P. 2008. Comparison between ultrasound and magnetic resonance imaging in assessment of fetal cytomegalovirus infection. Prenat Diagn 28:753–758. https://doi.org/10.1002/pd.2037.
18. Malinger G, Lev D, Zahalka N, Ben Aroia Z, Watemberg N, Kidron D, Sira LB, Lerman-Sagie T. 2003. Fetal cytomegalovirus infection of the brain: the spectrum of sonographic findings. Am J Neuroradiol 24:28–32.
19. Ishiwata M, Baba S, Kawashima M, Kosugi I, Kawasaki H, Kaneta M, Tsuchida T, Kozuma S, Tsutsui Y. 2006. Differential expression of the immediate-early 2 and 3 proteins in developing mouse brains infected with murine cytomegalovirus. Arch Virol 151:2181–2196. https://doi.org/10.1007/s00705-006-0793-0.
20. Enders G, Daiminger A, Bader U, Exler S, Enders M. 2011. Intrauterine transmission and clinical outcome of 248 pregnancies with primary cytomegalovirus infection in relation to gestational age. J Clin Virol 52:244–246. https://doi.org/10.1016/j.jcv.2011.07.005.
21. Stagno S, Pass RF, Cloud G, Britt WJ, Henderson RE, Walton PD, Veren DA, Page F, Alford CA. 1986. Primary cytomegalovirus infection in pregnancy. Incidence, transmission to fetus, and clinical outcome. JAMA 256:1904–1908.
22. Boppana S, Fowler KB. 2007. Persistence in the population: epidemiology and transmission, p 795–813. *In* Arvin AC-FG, Mocarski E, Roizman B, Whitley R, Yamanishi K (ed), Human herpesviruses: biology, therapy, and immunoprophylaxis. Cambridge, Cambridge, United Kingdom.
23. Becroft DM. 1981. Prenatal cytomegalovirus infection: epidemiology, pathology and pathogenesis. Perspect Pediatr Pathol 6:203–241.
24. Perlman JM, Argyle C. 1992. Lethal cytomegalovirus infection in preterm infants: clinical, radiological, and neuropathological findings. Ann Neurol 31:64–68. https://doi.org/10.1002/ana.410310112.
25. Gabrielli L, Bonasoni MP, Santini D, Piccirilli G, Chiereghin A, Petrisli E, Dolcetti R, Guerra B, Piccioli M, Lanari M, Landini MP, Lazzarotto T. 2012. Congenital cytomegalovirus infection: patterns of fetal brain damage. Clin Microbiol Infect 18:E419–E427. https://doi.org/10.1111/j.1469-0691.2012.03983.x.
26. Koontz T, Bralic M, Tomac J, Pernjak-Pugel E, Bantug G, Jonjic S, Britt WJ. 2008. Altered development of the brain after focal herpesvirus infection of the central nervous system. J Exp Med 205:423–435. https://doi.org/10.1084/jem.20071489.
27. Britt WJ, Cekinovic D, Jonjic S. 2013. Murine model of neonatal cytomegalovirus infection, p 119–141. *In* Reddehase M (ed), Cytomegaloviruses: from molecular pathogenesis to intervention, vol 2. Caister Academic Press, Norfolk, United Kingdom.
28. Bantug GR, Cekinovic D, Bradford R, Koontz T, Jonjic S, Britt WJ. 2008. CD8$^+$ T lymphocytes control murine cytomegalovirus replication in the central nervous system of newborn animals. J Immunol 181:2111–2123. https://doi.org/10.4049/jimmunol.181.3.2111.
29. Kosmac K, Bantug GR, Pugel EP, Cekinovic D, Jonjic S, Britt WJ. 2013. Glucocorticoid treatment of MCMV infected newborn mice attenuates CNS inflammation and limits deficits in cerebellar development. PLoS Pathog 9:e1003200. https://doi.org/10.1371/journal.ppat.1003200.
30. Heine VM, Rowitch DH. 2009. Hedgehog signaling has a protective effect in glucocorticoid-induced mouse neonatal brain injury through an 11betaHSD2-dependent mechanism. J Clin Invest 119:267–277.
31. Parikh NA, Lasky RE, Kennedy KA, Moya FR, Hochhauser L, Romo S, Tyson JE. 2007. Postnatal dexamethasone therapy and cerebral tissue volumes in extremely low birth weight infants. Pediatrics 119:265–272. https://doi.org/10.1542/peds.2006-1354.
32. Tam EW, Chau V, Ferriero DM, Barkovich AJ, Poskitt KJ, Studholme C, Fok ED, Grunau RE, Glidden DV, Miller SP. 2011. Preterm cerebellar growth impairment after postnatal exposure to glucocorticoids. Sci Transl Med 3:105ra105. https://doi.org/10.1126/scitranslmed.3002884.
33. Pavic I, Polic B, Crnkovic I, Lucin P, Jonjic S, Koszinowski UH. 1993. Participation of endogenous tumour necrosis factor alpha in host resistance to cytomegalovirus infection. J Gen Virol 74:2215–2223. https://doi.org/10.1099/0022-1317-74-10-2215.
34. Orange JS, Biron CA. 1996. Characterization of early IL-12, IFN-alphabeta, and TNF effects on antiviral state and NK cell responses during murine cytomegalovirus infection. J Immunol 156:4746–4756.
35. Heise MT, Pollock JL, O'Guin A, Barkon ML, Bormley S, Virgin HWT. 1998. Murine cytomegalovirus infection inhibits IFN gamma-induced MHC class II expression on macrophages: the role of type I interferon. Virology 241:331–344. https://doi.org/10.1006/viro.1997.8969.
36. Yerkovich ST, Olver SD, Lenzo JC, Peacock CD, Price P. 1997. The roles of tumour necrosis factor-alpha, interleukin-1 and interleukin-12 in murine cytomegalovirus infection. Immunology 91:45–52. https://doi.org/10.1046/j.1365-2567.1997.00226.x.
37. Cheeran MC, Hu S, Yager SL, Gekker G, Peterson PK, Lokensgard JR. 2001. Cytomegalovirus induces cytokine and chemokine production differentially in microglia and astrocytes: antiviral implications. J Neurovirol 7:135–147. https://doi.org/10.1080/13550280152058799.
38. Shrestha B, Zhang B, Purtha WE, Klein RS, Diamond MS. 2008. Tumor necrosis factor alpha protects against lethal West Nile virus infection by promoting trafficking of mononuclear leukocytes into the central nervous system. J Virol 82:8956–8964. https://doi.org/10.1128/JVI.01118-08.
39. Heise MT, Virgin HWT. 1995. The T-cell-independent role of gamma interferon and tumor necrosis factor alpha in macrophage activation during murine cytomegalovirus and herpes simplex virus infections. J Virol 69:904–909.
40. Lundberg P, Welander PV, Edwards CK III, van Rooijen N, Cantin E. 2007. Tumor necrosis factor (TNF) protects resistant C57BL/6 mice against herpes simplex virus-induced encephalitis independently of signaling via TNF receptor 1 or 2. J Virol 81:1451–1460. https://doi.org/10.1128/JVI.02243-06.
41. Suresh M, Gao X, Fischer C, Miller NE, Tewari K. 2004. Dissection of antiviral and immune regulatory functions of tumor necrosis factor receptors in a chronic lymphocytic choriomeningitis virus infection. J Virol 78:3906–3918. https://doi.org/10.1128/JVI.78.8.3906-3918.2004.
42. Wang T, Town T, Alexopoulou L, Anderson J, Fikrig E, Flavell RA. 2004. Toll-like receptor 3 mediates West Nile virus entry into the brain causing lethal encephalitis. Nat Med 10:1366–1373. https://doi.org/10.1038/nm1140.
43. Pulliam L, Herndier BG, Tang NM, McGrath MS. 1991. Human immunodeficiency virus-infected macrophages produce soluble factors that cause histological and neurochemical alterations in cultured human brains. J Clin Invest 87:503–512. https://doi.org/10.1172/JCI115024.
44. Ryan LA, Cotter RL, Zink WEII, Gendelman HE, Zheng J. 2002. Macrophages, chemokines and neuronal injury in HIV-1-associated dementia. Cell Mol Biol 48:137–150.
45. Ryan LA, Peng H, Erichsen DA, Huang Y, Persidsky Y, Zhou Y, Gendelman HE, Zheng J. 2004. TNF-related apoptosis-inducing ligand mediates human neuronal apoptosis: links to HIV-1-associated dementia. J Neuroimmunol 148:127–139. https://doi.org/10.1016/j.jneuroim.2003.11.019.

46. Talley AK, Dewhurst S, Perry SW, Dollard SC, Gummuluru S, Fine SM, New D, Epstein LG, Gendelman HE, Gelbard HA. 1995. Tumor necrosis factor alpha-induced apoptosis in human neuronal cells: protection by the antioxidant N-acetylcysteine and the genes bcl-2 and crmA. Mol Cell Biol 15:2359–2366. https://doi.org/10.1128/MCB.15.5.2359.
47. Yoshioka M, Bradley WG, Shapshak P, Nagano I, Stewart RV, Xin KQ, Srivastava AK, Nakamura S. 1995. Role of immune activation and cytokine expression in HIV-1-associated neurologic diseases. Adv Neuroimmunol 5:335–358. https://doi.org/10.1016/0960-5428(95)00012-Q.
48. Brabers NA, Nottet HS. 2006. Role of the pro-inflammatory cytokines TNF-alpha and IL-1beta in HIV-associated dementia. Eur J Clin Invest 36:447–458. https://doi.org/10.1111/j.1365-2362.2006.01657.x.
49. Nargi-Aizenman JL, Havert MB, Zhang M, Irani DN, Rothstein JD, Griffin DE. 2004. Glutamate receptor antagonists protect from virus-induced neural degeneration. Ann Neurol 55:541–549. https://doi.org/10.1002/ana.20033.
50. Ye L, Huang Y, Zhao L, Li Y, Sun L, Zhou Y, Qian G, Zheng JC. 2013. IL-1beta and TNF-alpha induce neurotoxicity through glutamate production: a potential role for neuronal glutaminase. J Neurochem 125:897–908. https://doi.org/10.1111/jnc.12263.
51. Probert L, Akassoglou K, Pasparakis M, Kontogeorgos G, Kollias G. 1995. Spontaneous inflammatory demyelinating disease in transgenic mice showing central nervous system-specific expression of tumor necrosis factor {alpha}. Proc Natl Acad Sci U S A 92:11294–11298. https://doi.org/10.1073/pnas.92.24.11294.
52. Kramer K, Schaudien D, Eisel UL, Herzog S, Richt JA, Baumgartner W, Herden C. 2012. TNF-overexpression in Borna disease virus-infected mouse brains triggers inflammatory reaction and epileptic seizures. PLoS One 7:e41476. https://doi.org/10.1371/journal.pone.0041476.
53. Lin KL, Suzuki Y, Nakano H, Ramsburg E, Gunn MD. 2008. CCR2$^+$ monocyte-derived dendritic cells and exudate macrophages produce influenza-induced pulmonary immune pathology and mortality. J Immunol 180:2562–2572. https://doi.org/10.4049/jimmunol.180.4.2562.
54. Lin KL, Sweeney S, Kang BD, Ramsburg E, Gunn MD. 2011. CCR2-antagonist prophylaxis reduces pulmonary immune pathology and markedly improves survival during influenza infection. J Immunol 186:508–515. https://doi.org/10.4049/jimmunol.1001002.
55. Hatten ME, Alder J, Zimmerman K, Heintz N. 1997. Genes involved in cerebellar cell specification and differentiation. Curr Opin Neurobiol 7:40–47. https://doi.org/10.1016/S0959-4388(97)80118-3.
56. Morales D, Hatten ME. 2006. Molecular markers of neuronal progenitors in the embryonic cerebellar anlage. J Neurosci 26:12226–12236. https://doi.org/10.1523/JNEUROSCI.3493-06.2006.
57. Ohshima T, Gilmore EC, Longenecker G, Jacobowitz DM, Brady RO, Herrup K, Kulkarni AB. 1999. Migration defects of cdk5(−/−) neurons in the developing cerebellum is cell autonomous. J Neurosci 19:6017–6026.
58. Kumazawa A, Mita N, Hirasawa M, Adachi T, Suzuki H, Shafeghat N, Kulkarni AB, Mikoshiba K, Inoue T, Ohshima T. 2013. Cyclin-dependent kinase 5 is required for normal cerebellar development. Mol Cell Neurosci 52:97–105. https://doi.org/10.1016/j.mcn.2012.10.007.
59. Ko J, Humbert S, Bronson RT, Takahashi S, Kulkarni AB, Li E, Tsai LH. 2001. p35 and p39 are essential for cyclin-dependent kinase 5 function during neurodevelopment. J Neurosci 21:6758–6771.
60. Ehler E, van Leeuwen F, Collard JG, Salinas PC. 1997. Expression of Tiam-1 in the developing brain suggests a role for the Tiam-1-Rac signaling pathway in cell migration and neurite outgrowth. Mol Cell Neurosci 9:1–12.
61. Zhou P, Porcionatto M, Pilapil M, Chen Y, Choi Y, Tolias KF, Bikoff JB, Hong EJ, Greenberg ME, Segal RA. 2007. Polarized signaling endosomes coordinate BDNF-induced chemotaxis of cerebellar precursors. Neuron 55:53–68. https://doi.org/10.1016/j.neuron.2007.05.030.
62. Cekinovic D, Golemac M, Pugel EP, Tomac J, Cicin-Sain L, Slavuljica I, Bradford R, Misch S, Winkler TH, Mach M, Britt WJ, Jonjic S. 2008. Passive immunization reduces murine cytomegalovirus-induced brain pathology in newborn mice. J Virol 82:12172–12180. https://doi.org/10.1128/JVI.01214-08.
63. Omi A, Enomoto Y, Kiniwa T, Miyata N, Miyajima A. 2014. Mature resting Ly6C(high) natural killer cells can be reactivated by IL-15. Eur J Immunol 44:2638–2647. https://doi.org/10.1002/eji.201444570.
64. Auffray C, Sieweke MH, Geissmann F. 2009. Blood monocytes: development, heterogeneity, and relationship with dendritic cells. Annu Rev Immunol 27:669–692. https://doi.org/10.1146/annurev.immunol.021908.132557.
65. Hanninen A, Maksimow M, Alam C, Morgan DJ, Jalkanen S. 2011. Ly6C supports preferential homing of central memory CD8$^+$ T cells into lymph nodes. Eur J Immunol 41:634–644. https://doi.org/10.1002/eji.201040760.
66. Hu Z, Blackman MA, Kaye KM, Usherwood EJ. 2015. Functional heterogeneity in the CD4$^+$ T cell response to murine gamma-herpesvirus 68. J Immunol 194:2746–2756. https://doi.org/10.4049/jimmunol.1401928.
67. Butovsky O, Siddiqui S, Gabriely G, Lanser AJ, Dake B, Murugaiyan G, Doykan CE, Wu PM, Gali RR, Iyer LK, Lawson R, Berry J, Krichevsky AM, Cudkowicz ME, Weiner HL. 2012. Modulating inflammatory monocytes with a unique microRNA gene signature ameliorates murine ALS. J Clin Invest 122:3063–3087. https://doi.org/10.1172/JCI62636.
68. Sedgwick JD, Schwender S, Imrich H, Dorries R, Butcher GW, ter Meulen V. 1991. Isolation and direct characterization of resident microglial cells from the normal and inflamed central nervous system. Proc Natl Acad Sci U S A 88:7438–7442. https://doi.org/10.1073/pnas.88.16.7438.
69. Mildner A, Mack M, Schmidt H, Bruck W, Djukic M, Zabel MD, Hille A, Priller J, Prinz M. 2009. CCR2+Ly-6Chi monocytes are crucial for the effector phase of autoimmunity in the central nervous system. Brain 132:2487–2500. https://doi.org/10.1093/brain/awp144.
70. Wilson EH, Weninger W, Hunter CA. 2010. Trafficking of immune cells in the central nervous system. J Clin Invest 120:1368–1379. https://doi.org/10.1172/JCI41911.
71. Ajami B, Bennett JL, Krieger C, McNagny KM, Rossi FM. 2011. Infiltrating monocytes trigger EAE progression, but do not contribute to the resident microglia pool. Nat Neurosci 14:1142–1149. https://doi.org/10.1038/nn.2887.
72. Katsumoto A, Lu H, Miranda AS, Ransohoff RM. 2014. Ontogeny and functions of central nervous system macrophages. J Immunol 193:2615–2621. https://doi.org/10.4049/jimmunol.1400716.
73. Lim JK, Obara CJ, Rivollier A, Pletnev AG, Kelsall BL, Murphy PM. 2011. Chemokine receptor Ccr2 is critical for monocyte accumulation and survival in West Nile virus encephalitis. J Immunol 186:471–478. https://doi.org/10.4049/jimmunol.1003003.
74. Cusick MF, Libbey JE, Patel DC, Doty DJ, Fujinami RS. 2013. Infiltrating macrophages are key to the development of seizures following virus infection. J Virol 87:1849–1860. https://doi.org/10.1128/JVI.02747-12.
75. Yamasaki R, Lu H, Butovsky O, Ohno N, Rietsch AM, Cialic R, Wu PM, Doykan CE, Lin J, Cotleur AC, Kidd G, Zorlu MM, Sun N, Hu W, Liu L, Lee JC, Taylor SE, Uehlein L, Dixon D, Gu J, Floruta CM, Zhu M, Charo IF, Weiner HL, Ransohoff RM. 2014. Differential roles of microglia and monocytes in the inflamed central nervous system. J Exp Med 211:1533–1549. https://doi.org/10.1084/jem.20132477.
76. Auffray C, Emre Y, Geissmann F. 2008. Homeostasis of dendritic cell pool in lymphoid organs. Nat Immunol 9:584–586. https://doi.org/10.1038/ni0608-584.
77. Saijo K, Crotti A, Glass CK. 2013. Regulation of microglia activation and deactivation by nuclear receptors. Glia 61:104–111. https://doi.org/10.1002/glia.22423.
78. Horiuchi T, Mitoma H, Harashima S, Tsukamoto H, Shimoda T. 2010. Transmembrane TNF-alpha: structure, function and interaction with anti-TNF agents. Rheumatology 49:1215–1228. https://doi.org/10.1093/rheumatology/keq031.
79. Mitoma H, Horiuchi T, Tsukamoto H, Tamimoto Y, Kimoto Y, Uchino A, To K, Harashima S, Hatta N, Harada M. 2008. Mechanisms for cytotoxic effects of anti-tumor necrosis factor agents on transmembrane tumor necrosis factor alpha-expressing cells: comparison among infliximab, etanercept, and adalimumab. Arthritis Rheum 58:1248–1257. https://doi.org/10.1002/art.23447.
80. Ramesh G, MacLean AG, Philipp MT. 2013. Cytokines and chemokines at the crossroads of neuroinflammation, neurodegeneration, and neuropathic pain. Mediators Inflamm 2013:480739. https://doi.org/10.1155/2013/480739.
81. Strauss M, Griffith BP. 1991. Guinea pig model of transplacental congenital cytomegalovirus infection with analysis for labyrinthitis. Am J Otol 12:97–100.
82. Griffith BP, Aquino-de Jesus MJ. 1991. Guinea pig model of congenital cytomegalovirus infection. Transplant Proc 23:29–31.
83. Booss J, Dann PR, Griffith BP, Kim JH. 1988. Glial nodule encephalitis in the guinea pig: serial observations following cytomegalovirus infection. Acta Neuropathol 75:465–473. https://doi.org/10.1007/BF00687133.
84. Griffith BP, Hsiung GD. 1980. Cytomegalovirus infection in guinea pigs. IV. Maternal infection at different stages of gestation. J Infect Dis 141:787–793.

85. Clancy B, Darlington RB, Finlay BL. 2001. Translating developmental time across mammalian species. Neuroscience 105:7–17. https://doi.org/10.1016/S0306-4522(01)00171-3.
86. Bardina SV, Michlmayr D, Hoffman KW, Obara CJ, Sum J, Charo IF, Lu W, Pletnev AG, Lim JK. 2015. Differential roles of chemokines CCL2 and CCL7 in monocytosis and leukocyte migration during West Nile virus infection. J Immunol 195:4306–4318. https://doi.org/10.4049/jimmunol.1500352.
87. Wikstrom ME, Khong A, Fleming P, Kuns R, Hertzog PJ, Frazer IH, Andoniou CE, Hill GR, Degli-Esposti MA. 2014. The early monocytic response to cytomegalovirus infection is MyD88 dependent but occurs independently of common inflammatory cytokine signals. Eur J Immunol 44:409–419. https://doi.org/10.1002/eji.201243109.
88. Drevets DA, Schawang JE, Dillon MJ, Lerner MR, Bronze MS, Brackett DJ. 2008. Innate responses to systemic infection by intracellular bacteria trigger recruitment of Ly-6Chigh monocytes to the brain. J Immunol 181:529–536. https://doi.org/10.4049/jimmunol.181.1.529.
89. Serbina NV, Shi C, Pamer EG. 2012. Monocyte-mediated immune defense against murine Listeria monocytogenes infection. Adv Immunol 113:119–134. https://doi.org/10.1016/B978-0-12-394590-7.00003-8.
90. Jia T, Serbina NV, Brandl K, Zhong MX, Leiner IM, Charo IF, Pamer EG. 2008. Additive roles for MCP-1 and MCP-3 in CCR2-mediated recruitment of inflammatory monocytes during Listeria monocytogenes infection. J Immunol 180:6846–6853. https://doi.org/10.4049/jimmunol.180.10.6846.
91. Tsou CL, Peters W, Si Y, Slaymaker S, Aslanian AM, Weisberg SP, Mack M, Charo IF. 2007. Critical roles for CCR2 and MCP-3 in monocyte mobilization from bone marrow and recruitment to inflammatory sites. J Clin Invest 117:902–909. https://doi.org/10.1172/JCI29919.
92. Chen BP, Kuziel WA, Lane TE. 2001. Lack of CCR2 results in increased mortality and impaired leukocyte activation and trafficking following infection of the central nervous system with a neurotropic coronavirus. J Immunol 167:4585–4592. https://doi.org/10.4049/jimmunol.167.8.4585.
93. Izikson L, Klein RS, Charo IF, Weiner HL, Luster AD. 2000. Resistance to experimental autoimmune encephalomyelitis in mice lacking the CC chemokine receptor (CCR)2. J Exp Med 192:1075–1080. https://doi.org/10.1084/jem.192.7.1075.
94. Bennett JL, Elhofy A, Charo I, Miller SD, Dal Canto MC, Karpus WJ. 2007. CCR2 regulates development of Theiler's murine encephalomyelitis virus-induced demyelinating disease. Viral Immunol 20:19–33. https://doi.org/10.1089/vim.2006.0068.
95. Serbina NV, Jia T, Hohl TM, Pamer EG. 2008. Monocyte-mediated defense against microbial pathogens. Annu Rev Immunol 26:421–452. https://doi.org/10.1146/annurev.immunol.26.021607.090326.
96. Kigerl KA, Gensel JC, Ankeny DP, Alexander JK, Donnelly DJ, Popovich PG. 2009. Identification of two distinct macrophage subsets with divergent effects causing either neurotoxicity or regeneration in the injured mouse spinal cord. J Neurosci 29:13435–13444. https://doi.org/10.1523/JNEUROSCI.3257-09.2009.
97. Suthar MS, Diamond MS, Gale M, Jr. 2013. West Nile virus infection and immunity. Nat Rev Microbiol 11:115–128. https://doi.org/10.1038/nrmicro2950.
98. Getts DR, Terry RL, Getts MT, Muller M, Rana S, Shrestha B, Radford J, Van Rooijen N, Campbell IL, King NJ. 2008. Ly6c+ "inflammatory monocytes" are microglial precursors recruited in a pathogenic manner in West Nile virus encephalitis. J Exp Med 205:2319–2337. https://doi.org/10.1084/jem.20080421.
99. Getts DR, Terry RL, Getts MT, Deffrasnes C, Muller M, van Vreden C, Ashhurst TM, Chami B, McCarthy D, Wu H, Ma J, Martin A, Shae LD, Witting P, Kansas GS, Kuhn J, Hafezi W, Campbell IL, Reilly D, Say J, Brown L, White MY, Cordwell SJ, Chadban SJ, Thorp EB, Bao S, Miller SD, King NJ. 2014. Therapeutic inflammatory monocyte modulation using immune-modifying microparticles. Sci Transl Med 6:219ra7. https://doi.org/10.1126/scitranslmed.3007563.
100. Shrestha B, Diamond MS. 2004. Role of CD8+ T cells in control of West Nile virus infection. J Virol 78:8312–8321. https://doi.org/10.1128/JVI.78.15.8312-8321.2004.
101. Netland J, Bevan MJ. 2013. CD8 and CD4 T cells in West Nile virus immunity and pathogenesis. Viruses 5:2573–2584. https://doi.org/10.3390/v5102573.
102. Chastain EM, Getts DR, Miller SD. 2015. Deficient natural killer dendritic cell responses underlay the induction of Theiler's virus-induced autoimmunity. mBio 6:e01175. https://doi.org/10.1128/mBio.01175-15.
103. Dungan LS, McGuinness NC, Boon L, Lynch MA, Mills KH. 2014. Innate IFN-gamma promotes development of experimental autoimmune encephalomyelitis: a role for NK cells and M1 macrophages. Eur J Immunol 44:2903–2917. https://doi.org/10.1002/eji.201444612.
104. Trifilo MJ, Montalto-Morrison C, Stiles LN, Hurst KR, Hardison JL, Manning JE, Masters PS, Lane TE. 2004. CXC chemokine ligand 10 controls viral infection in the central nervous system: evidence for a role in innate immune response through recruitment and activation of natural killer cells. J Virol 78:585–594. https://doi.org/10.1128/JVI.78.2.585-594.2004.
105. Wang T, Welte T. 2013. Role of natural killer and gamma-delta T cells in West Nile virus infection. Viruses 5:2298–2310. https://doi.org/10.3390/v5092298.
106. Marcoe JP, Lim JR, Schaubert KL, Fodil-Cornu N, Matka M, McCubbrey AL, Farr AR, Vidal SM, Laouar Y. 2012. TGF-beta is responsible for NK cell immaturity during ontogeny and increased susceptibility to infection during mouse infancy. Nat Immunol 13:843–850. https://doi.org/10.1038/ni.2388.
107. Thongtan T, Thepparit C, Smith DR. 2012. The involvement of microglial cells in Japanese encephalitis infections. Clin Dev Immunol 2012:890586. https://doi.org/10.1155/2012/890586.
108. Conrady CD, Zheng M, van Rooijen N, Drevets DA, Royer D, Alleman A, Carr DJ. 2013. Microglia and a functional type I IFN pathway are required to counter HSV-1-driven brain lateral ventricle enlargement and encephalitis. J Immunol 190:2807–2817. https://doi.org/10.4049/jimmunol.1203265.
109. Hong S, Banks WA. 2015. Role of the immune system in HIV-associated neuroinflammation and neurocognitive implications. Brain Behav Immun 45:1–12. https://doi.org/10.1016/j.bbi.2014.10.008.
110. Rasband W. 1997–2012. ImageJ. NIH, Bethesda, MD.